62-4-6

Copy 53

USL Report No. 559
1-052-00-00

WALL PRESSURE CORRELATIONS IN TURBULENT PIPE FLOW

S-R011 01 01-0401

20 August 1962

by

Henry P. Bakewell, Jr.
George F. Carey
John J. Libuha
Howard H. Schloemer
and
William A. Von Winkle

U. S. NAVY UNDERWATER SOUND LABORATORY
FORT TRUMBULL NEW LONDON, CONNECTICUT

ABSTRACT

Certain properties of the pressure field induced by turbulent airflow at the wall of a cylindrical pipe have been investigated over broad frequency bands and in octave frequency bands over a limited range of Reynolds numbers. The broad-band measurements indicate that the pressure field is convected downstream at approximately 0.7 of the centerline velocity. The ratio of the root-mean-square pressure to the dynamic pressure is approximately equal to 0.006 for the various Reynolds numbers. Longitudinal and lateral space correlations are also presented for a limited range of spatial separations. Data obtained in octave frequency bands indicate that the ratio of convection velocity to centerline velocity decreases as frequency increases, with the ratio varying from approximately unity to 0.64 for the frequency bands investigated. Longitudinal and lateral correlation data for various frequencies, spatial separations, and Reynolds numbers are shown to be functions of Strouhal number. Estimates of the longitudinal and lateral scales are given as functions of frequency for the various Reynolds numbers. These data indicate that the lateral scale is approximately equal to one half of the longitudinal scale.

ADMINISTRATIVE INFORMATION

The work described in this report was initiated in May 1960 by Dr. William A. Von Winkle and was carried out under USL Job Orders Nos. 1-612-07-00 and 1-052-00-0C and Navy Project No. S-k011 01 01-0401.

Dr. Von Winkle prepared the program planning specification and supervised the design, construction, and preliminary check-out of the turbulent pipe flow facility until September 1961, when he was appointed USL Representative for a special program at Bermuda. He has continued to serve the project in a consultant capacity.

George F. Carey, who had designed the facility and had guided the project throughout the construction and check-out stages, assumed Dr. Von Winkle's supervisory duties.

Howard H. Schloemer, Assistant Professor of Mechanical Engineering at the City College, New York, and a member of the USL staff for the past three summers, assisted in the preliminary design of the tunnel and obtained the initial wall pressure correlation data.

Henry P. Bakewell, Jr., and John J. Libuba obtained the data reported in this study. In addition, Mr. Bakewell performed the mathematical analysis of the experimental results, and Mr. Libuba assembled and modified existing instrumentation for the pipe flow facility.

REVIEWED AND APPROVED: 20 AUGUST 1962

J. Warren Horton
Technical Director

B. H. Arnold, Captain, USN
Commanding Officer and Director

TABLE OF CONTENTS

LIST OF ILLUSTRATIONS

LIST OF ILLUSTRATIONS (Cont'd)

LIST OF TABLES

SYMBOLS

d	Pipe diameter
f	Frequency in cycles per second
$p(x, y, t)$	Fluctuating pressure
r	Active radius of transducer face
R	Reynolds number based on pipe diameter
t	Time
τ	Time delay
u_{d_c}	Centerline pipe velocity
u_{conv}	Convection velocity
x, y	Longitudinal and lateral space coordinates
ξ, η	Longitudinal and lateral separation of transducers
ω	Angular frequency
S	Strouhal number
$\psi(\xi, \eta, \tau)$	Normalized space-time correlation function
ρ	Fluid density
J_n	Bessel function of the first kind of order n
λ_ξ	Longitudinal scale
λ_η	Lateral scale

$Y(f) = \dfrac{\overline{P_i^2}}{\overline{\text{BANDWIDTH}}}$ where $\overline{P_i^2}$ is the mean square pressure within a third octave band

δ	Boundary layer thickness

WALL PRESSURE CORRELATIONS IN TURBULENT PIPE FLOW

INTRODUCTION

Certain properties of the turbulent pressure field at the wall of a cylindrical pipe have been investigated experimentally over a range of Reynolds numbers from 100,000 to 300,000. In particular, data have been obtained concerning the convection velocity and longitudinal space-time correlations both over broad frequency bands and in octave bands. Longitudinal and lateral correlations have also been obtained over broad bands as functions of spatial separation and in octave bands as functions of Strouhal number. Finally, measurements of the root-mean-square pressures and the frequency spectra have been made.

GENERAL DESCRIPTION OF THE TUNNEL

The turbulent pipe flow facility is located in the massive old fort at the Point Trumbull site of the Underwater Sound Laboratory. This location was selected because of its low ambient noise level and solid, vibration-free foundation.

The development of the experimental apparatus, Fig. 1, which was used in this investigation began with the work of Von Winkle and Weyers.[1] Knowledge of the deficiencies of the apparatus used in their investigations was of considerable help in the design of the present system.

Blower noise was attenuated by shock-mounting the blower frame, encasing it in a plywood box lined with six inches of superfine fiberglass insulation, and using a large muffler at the exit of the blower. This muffler was found to act effectively as a low-pass acoustic filter with a cutoff frequency of 80 cps. In addition, the blower was decoupled from the muffler by a 3-foot-long section of neoprene tubing wrapped with fiberglass. A short length of rubber tubing connected this upstream muffler with the pipe.

A 40-foot-long brass pipe of 3.5-inch inside diameter and 4.5-inch outside diameter is the major component of the experimental system. The pipe is supported on small, rubber-lined, wooden blocks which are fastened

---

[1] W. A. VonWinkle, Some Measurements of Longitudinal Space-Time Correlations of Wall Pressure Fluctuations in Turbulent Pipe Flow, USL Report No. 528, 17 August 1961; and P. F. R. Weyers, The Vibration and Acoustic Radiation of Thin-Walled Cylinders Caused by Internal Turbulent Flow, Guggenheim Aeronautical Laboratory Report on Contract NAw-6517, August 1958.

on top of large wooden tables. Except for the test section, this pipe is entirely encased in a 12-inch by 12-inch sand-filled plywood box. Tests using an accelerometer mounted on the pipe wall at the test section indicated that the pipe was free of resonances. A downstream muffler was also provided to attenuate any pressure fluctuations resulting in the mixing of the exhaust stream with ambient air.

The test section itself was located 96 pipe diameters downstream of the upstream muffler to insure fully developed turbulent flow. A traversing mechanism which allowed interchangeable use of Pitot tubes, stagnation and static pressure probes, and hot wire probes was used to determine the velocity distribution across the pipe. The resulting 1/8 power law velocity distribution, obtained from Pitot tube traverses, confirmed other measurements and indicated that the turbulent flow was fully developed.[2]

Static pressure taps were located 9 feet apart along the length of the pipe upstream of the test section to measure differential pressure. The velocity of the flow was monitored by observing this pressure differential on a draft gauge. Changes in velocity were accomplished by moving a damper in the inlet of the blower. A remotely controlled drive mechanism was used to control the damper from the test section location.

The range of mean velocities available for the experiment extended from 60 ft/sec to 178 ft/sec. This corresponded to a Reynolds number range, based on pipe diameter, of 100,000 to 300,000.

Compressibility effects were ignored since the highest local Mach number, at a centerline velocity of 214 ft/sec, is 0.185, well below the nominal three-tenths Mach number generally used as the lower limit of compressibility phenomena.

The test section was a 2-foot-long section of pipe, which could be removed from the pipe run and replaced by other sections (such as an anechoic chamber). For measurements of pressure fluctuations a 1.5-inch-diameter hole was drilled in the pipe, into which brass plugs could be inserted.

A series of 0.1525-inch-diameter holes in each plug allowed interchangeable use of transducers and dummy sections with the result that many different combinations of spacings could be obtained with only two transducers.

---

[2] For a discussion of fully developed turbulent pipe flow, see H. Schlichting, Boundary Layer Theory, McGraw-Hill Book Co., Inc., New York, 1955.

Different brass plugs were used to obtain longitudinal and lateral space correlations. Tolerances of the assembled system were kept close to ensure no protrusions of greater than 0.001 inches into the air stream. This value corresponded to approximately half the calculated thickness of the laminar sub-layer.

INSTRUMENTATION

The active face radius of the transducer element was taken as 110 percent of the actual radius of the active element. The resulting active transducer radius was only 0.0344 inches—51 times smaller than the pipe radius of 1.75 inches.

The computed longitudinal and lateral scales were 0.15 and 0.075 inches, respectively, which were 4.36 and 2.18 times larger than the active transducer radius. Since the squares of the recipocals of the last two ratios were dominant in the corrections for finite transducer size, these correction factors were very small, as is noted in Figs. 3, 4 and 5.

The transducers were constructed of a lead zirconate ceramic in a manner very similar to the types used by Franz and by Barger and Von Winkle[3] in their investigations of boundary layer pressure fluctuations The electrical characteristics of a typical transducer are as follows:

nominal sensitivity:	-120db//1v/μb, or 1μv/μbar
nominal frequency range:	90 cps to 20 kc
nominal capacitance:	40μμf

The transducers were essentially free-field calibrated over a frequency range of from 90 cps to 20 kc. The open-circuit receiving sensitivity response was reasonably flat and was approximately -120 db//1v/μb. To minimize loading losses for this high-impedance source, a one-inch length of Microdot connecting cable and a specially modified Endevco model 2607 amplifier were used to accommodate the high impedarce of the transducer. This transducer-preamplifier combination satisfactorily amplified the low-level signal from the transducer to a level sufficient for analysis and recording.

---

[3] G. J. Franz, "Turbulent Boundary-Layer Pressure Fluctuations on the Bow Dome and Superstructure of the USS ALBACORE (AGSS 569)," U. S. Navy Journal of Underwater Acoustics, vol. XII, no. 1, January 1962 (CONFIDENTIAL); and J. A. Barger and W. A. VonWinkle, "An Evaluation of a Boundary Layer Stabilization Coating," a paper presented at the sixty-first meeting of the Acoustical Society of America in Philadelphia, Pa., on 10-13 May 1961.

The measurement system, Fig. 2, consisted of two identical channels of instrumentation. Each channel contained an LDX-107 transducer and matching Endevco amplifier, a Daven decade attenuator, a Burr-Brown amplifier, a Gertsch 1/2 octave filter set, and a Ballantine amplifier. The outputs of the two channels were used as inputs to the polarity coincidence correlator either directly or through a dual-channel Ampex tape recorder with a variable time delay. Also incorporated into the system for spectrum analysis of the noise signal were a Brüel and Kjaer 1/3 octave frequency analyzer and a Brüel and Kjaer proportional band analyzer. All instrumentation except the correlator, analyzers, and tape recorder were battery-powered to minimize electromagnetic radiation interference from external AC power sources and to minimize grounding problems.

A calibration of each channel showed the system response to be linear and flat from 40 cps to 40 kc and also to be in phase throughout the frequency range of interest. The correlator used was of the polarity coincidence type designed by the Naval Ordnance Laboratory as Model WOX-3A. All correlation measurements were later converted from the polarity coincidence correlator values to true correlation coefficients. Stability over long periods of time and dependence on the phase rather than the amplitude of the input signals were the major advantages of this instrument Since a signal input of 3 volts rms or greater was required to produce correct results, care was taken to ensure that the input signal exceeded this value and also that there was an adequate signal-to-noise ratio. Normally the input signal was placed at about 10 volts rms, which afforded a minimum of 13 db signal-to-noise ratio. No measurements were made in the portion of the spectrum where the ratio was below this value.

For the space correlation measurements, the generated signals were transmitted directly from the last stage of amplification into the correlator. For the space-time correlation measurements, the generated signals were recorded on a dual-channel tape recorder and played back through the variable time delay unit into the correlator. A system was then available which afforded maximum ease, flexibility, and reliability for making these measurements.

MEASUREMENTS

Root-Mean-Square Pressure, Pressure Coefficient, and Correction Factors

The pressure fluctuations were detected by using a wall-mounted transducer and were measured in 1/3 octave bands. The sound pressure level was calculated from these measurements by using the bandwidth corrections and calibration constants.

Root-mean-square pressures at each Reynolds number were obtained by averaging the sound pressure level in 1/3 octave bands, i.e.,

$$\sqrt{\overline{p_m^2}} = \sqrt{\sum_{i=1}^{N} \overline{p_i^2}}$$

where

N = the number of bands

and

$\overline{p_i^2}$ = the mean-square 1/3 octave band pressures.

The working frequency range was determined by signal-to-noise ratio rather than transducer response.

The root-mean-square pressure is displayed in Fig. 3 as a function of centerline velocity. It should be noted that the corrected values are very near the measured quantities because of the small size of the transducers.

The correction factor[4] used is

$$\frac{\overline{p_m^2}}{\overline{p^2}} = 1 - \frac{A}{4\pi}\left(\frac{2}{\lambda_\xi^2} + \frac{2}{\lambda_\eta^2}\right)$$

---

[4] G. M. Corcos, J. W. Cuthbert, and W. A. VonWinkle, On the Measurement of Turbulent Pressure Fluctuations with a Transducer of Finite Size, University of California Berkeley, Institute of Engineering Research Report Series 82, Issue No. 12, November 1959, p. 23.

where

$\overline{p^2}$ and $\overline{p_m{}^2}$ = actual pressure and measured pressure, respectively,

and

A = effective area of transducer face.

Elsewhere in this report it is shown that $\lambda_\eta \cong 0.5\lambda_\xi$; hence, the correction factor reduces to

$$\sqrt{\frac{\overline{p_m^2}}{\overline{p^2}}} = \sqrt{1 - \frac{5}{2}\frac{r^2}{\lambda^2_\xi}} = 0.936$$

where r = 0.0344 inches and λ_ξ = 0.15 inches computed on a broad-band basis.

A plot of pressure coefficient versus Reynolds number is presented in Fig. 4. These values of the pressure coefficient are within the range of values reported by other investigators.[5] The slightly higher values found at the lower Reynolds numbers are due to the experimental scatter in the spectral values of the low-frequency components at these Reynolds numbers.

Frequency Spectrum

The non-dimensionalized frequency spectrum is shown in Fig. 5, which is in general agreement with the results of other investigators.[6] Again, the correction factor is small for most of the experimental range because of small values of r/λ_η. The correction factor[7] used is of the form

---

[5] VonWinkle, op. cit.; W. W. Willmarth, "Space-Time Correlations and Spectra of Wall Pressure in a Turbulent Boundary Layer," National Aeronautics and Space Administration Memorandum No. 3/17/59W, March 1959; D. H. Tack, M. W. Smith, and R. F. Lambert, "Wall Pressure Correlations in Turbulent Airflow," Journal of the Acoustical Society of America, vol. 33, no. 4, April 1961; and G. M. Corcos and W. A. VonWinkle "Some Measurements of the Presure Field at the Boundary of a Fully Developed Pipe Flow," a paper presented at the 1959 Divisional Meeting of the Division of Fluid Mechanics of the American Physical Society, at Ann Arbor, Mich., on 23-25 November 1959.

[6] VonWinkle, op. cit.; Willmarth, op. cit.; Franz, op. cit.; and M. Harrison, Pressure Fluctuations on the Wall Adjacent to a Turbulent Boundary Layer, David Taylor Model Basin Report No. 1260, December 1958.

[7] Corcos, Cuthbert, and VonWinkle, op. cit., p. 21.

$$\frac{\phi_m(\omega)}{\phi(\omega)} = \frac{4}{y^2}\left[J_1^2(y) + 2K_2 r^2 \frac{J_1(y)J_2(y)}{y} + 6K_4 r^4 \frac{(J_1(y)J_3(y) + J_2^2(y))}{y^2} + \cdots\right]$$

with

$$K_{2n} = \frac{1}{(2n)!}\left[\frac{\partial^{2n}\psi}{\partial\eta^{2n}}\right]_{\eta=0}$$

and

$$y = \frac{r\omega}{u_{conv}}$$

For the data in question only the first two terms are necessary, with the second term in the order of 10 percent of the first term.

Using the generally accepted definition of scale, i.e., $\frac{\partial^2\psi}{\partial\eta^2} = -\frac{2}{\lambda_\eta^2}$ and $\lambda_\eta \cong 0.5\lambda_\xi$ along with other constants previously mentioned, the correction factor equation reduces to

$$\frac{\phi_m(\omega)}{\phi(\omega)} = \frac{4}{y^2}J_1^2(y) - \frac{1.5862}{y^3}J_1(y)J_2(y).$$

This is displayed in Fig. 6. The corrected spectral values lie within experimental scatter over a wide range of non-dimensional frequencies, as is seen by inspection of Fig. 5.

The Convection Velocity

Space-time correlation measurements of the pressure fluctuations at the wall have been made in octave bands and in broad bands by recording the signals from two transducers at various longitudinal separations and then introducing time delay mechanically between the two channels during playback. The recorded trace of the cross-correlogram shows a maximum value at a finite value of time delay τ_c (measured from zero of time delay). The rate at which the pressure field at the wall is convected downstream is determined by dividing the longitudinal separation of the transducers by the time delay necessary to obtain a maximum of correlation.

The measurements of convection velocity were made at the following Reynolds numbers over the broad frequency bands indicated. (The upper limiting frequency in each case was determined by signal-to-noise ratio.)

Reynolds Number	Frequency Band
100,000	212-4800 cps
150,000	212-6800 cps
200,000	212-13,600 cps
250,000	212-20,000 cps
300,000	212-20,000 cps

Also at each Reynolds number, measurements of convection velocity were made in as many of the following octave bands as possible:

212-425 cps
425-850 cps
850-1700 cps
1700-3400 cps
3400-6800 cps
6800-13,600 cps

The ratio of the broad-band convection velocity to the centerline velocity has been determined and plotted against the Reynolds number in Fig. 7. This ratio has the value of approximately 0.70 and appears to be independent of Reynolds number. Although this value is lower than the 0.80 generally reported by other investigators,[8] it is consistently repeatable. It is possible that less averaging of the pressure fluctuations occurs because of the small ratio of the diameter of the active face of the transducer to the boundary layer thickness; $\frac{2r}{\delta} = \frac{2r}{d/2} = 0.039$.

The ratio of the convection velocity to the centerline velocity has also been determined in octave bands and plotted as a function of the geometric mean center frequency of each band in Fig. 8. The data for the different Reynolds numbers have been averaged together, as this ratio does not appear to depend on Reynolds number within each octave band. It is of interest that the pressure fluctuations, at the wall, of frequencies within the octave band centered at 300 cps are convected downstream at approximately the centerline velocity.

[8] VonWinkle, Harrison, Willmarth, and Tack, Smith, and Lambert; also M. K. Bull, Instrumentation for and Preliminary Measurements of Space-Time Correlations and Convection Velocities of the Pressure Field of a Turbulent Boundary Layer, University of Southampton (England) AASU Report No. 149, August 1960.

These data substantiate the theory that the ratio of convection velocity to centerline velocity decreases as the frequency increases with the ratio varying from approximately unity to 0.64 for the frequency bands investigated.

Investigations in the lateral direction, as expected, revealed no detectable convection velocity.

Decay Rate of the Correlation Maxima

A series of space-time correlations was made over a limited range of longitudinal transducer separations up to a maximum of 0.924 inches at a Reynolds number of 300,000 in octave bands and over the broad band 212-20,000 cps. The broad-band cross-correlograms are plotted against time delay τ in Fig. 9, indicating the rate of decay of the correlation maxima. The octave-band cross-correlograms are presented in a similar manner in Figs. 10 through 15 and indicate a small rate of decay of the low-frequency pressure fluctuations as compared with that of the higher-frequency components.

Longitudinal Space-Time Correlation

The same series of space-time correlations used to determine decay rates has been plotted against the parameter $\frac{\tau u_{conv}}{\xi}$ in octave frequency bands and over the broad band 212-20,000 cps at a Reynolds number of 300,000. These data are presented in Fig. 16 for the broad-band measurements and Figs. 17 through 22 for the octave-band measurements. For the various combinations of transducer separations and frequency bands all the correlation maxima occur at a value of approximately 1.0 for the parameter $\frac{\tau u_{conv}}{\xi}$ with the values of the maxima depending on the transducer separation ξ. (The higher values of correlation correspond to the smaller longitudinal separations ξ.) The slight deviations from the value of 1.0 for the parameter $\frac{\tau u_{conv}}{\xi}$ at the correlation maxima are due to the use of the average value of u_{conv} within a given frequency band instead of the individual value of u_{conv} determined for each cross-correlogram.

Longitudinal and Lateral Broad-Band Space Correlation

The normalized space-time correlation function of the fluctuating pressure is defined as

$$\psi(\xi,\eta,\tau) = \frac{\overline{P(x,y,t)\cdot p(x+\xi,y+\eta,t+\tau)}}{\overline{p^2(x,y,t)}} .$$

The longitudinal and lateral space correlation functions are special cases of the space-time correlation function $\psi(\xi,\eta,\tau)$ and are given respectively by $\psi(\xi,o,o)$ and $\psi(o,\eta,o)$. These functions have been obtained experimentally over the broadest frequency band available at each Reynolds number for transducer separations of 0.1515 to 0.9010 inches laterally and 0.276 to 0.924 inches longitudinally. The longitudinal and lateral space correlation data are plotted against the ratios of transducer separation to pipe radius, $\xi/d/2$ and $\eta/d/2$, respectively, in Figs. 23 through 27. As can be seen from the figures, the smallest available transducer separations are not sufficiently small to provide detailed information about the space correlation functions in the regions of $0<\xi/d/2<0.1$ and $0<\eta/d/2<0.1$. Thus, at the present time, no estimates of the broad-band lateral and longitudinal scales of the turbulence have been obtained from parabolic approximations of the space correlation curves. (Other estimates of scale will be discussed later.)

The interesting aspect of these data is that at each Reynolds number investigated, for equal values of longitudinal and lateral separation, the lateral space correlation has a higher value than the longitudinal correlation;

$$\psi(o,\eta,o) > \psi(\xi,o,o,) \quad \text{when} \quad \eta = \xi .$$

However, at closer separations than those investigated this relationship may not be true. Also, it should be noted that for a given transducer separation the values of the longitudinal and lateral space correlation functions appear to decrease as the Reynolds number is decreased.

Longitudinal and Lateral Correlation as Functions of Strouhal Number

Space correlation data were also obtained in octave frequency bands using the previously mentioned Reynolds numbers and longitudinal and lateral transducer separations. The functions which have been measured are special

cases of a correlation function of the type:

$$\psi_{f_o,R}(\xi,\eta,\tau) = \frac{\overline{P_{f_o,R}(x,y,t)\cdot P_{f_o,R}(x+\xi,y+\eta,t+\tau)}}{\overline{P^2}_{f_o,R}(x,y,t)}$$

The subscript f_o represents the geometric mean center frequency of the octave band, and the subscript R indicates the Reynolds number for a given measurement. The following table indicates the octave bands used.

Table 1

OCTAVE BANDS UTILIZED AT SPECIFIC REYNOLDS NUMBERS

Δf(cps)	f_o			
212-425	300	R = 100,000	R = 150,000	R = 200,000
425-850	600			R = 250,000
850-1700	1200			R = 300,000
1700-3400	2400			
3400-6800	4800			
6800-13,600	9600			

The longitudinal correlation function $\psi_{f_o,R}(\xi,o,o)$ and the lateral correlation function $\psi_{f_o,R}(o,\eta,o)$ have been determined experimentally and plotted against the Strouhal number $\left(S = \frac{f_o\zeta}{u_{c_L}} \text{ and } S = \frac{f_o\eta}{u_{c_L}}\right)$ in Figs. 28 and 30. The same functions have also been plotted against the Strouhal number with the frequency-dependent convection velocity in the denominator instead of the centerline velocity in Figs. 29 and 31.

The longitudinal correlation data for all Reynolds numbers, frequencies, and separations investigated appear to define a single curve similar to a damped cosine curve:

$$\psi_{f_o,R}(\zeta,o,o) \cong \cos(aS)e^{-bS^2}.$$

This type of curve can be fitted to the data almost up to the third zero of the function.

The lateral data for all Reynolds numbers, frequencies, and separations

investigated combine to define a single curve of the following nature:

$$\psi_{f_o,R}(o,\eta,o) \cong (1 + cS^2)^{-1} (2 - e^{-ds^2})^{-1} .$$

The values of the constants used in these mathematical expressions for longitudinal and lateral correlation functions are given below for both sets of data plotted against Strouhal number based on either convection velocity or centerline velocity.

Table 2

VALUES OF CONSTANTS IN CORRELATION EXPRESSIONS

Constants		Strouhal Number	Figure No.
$a = \frac{\pi}{2}\left(\frac{1}{.18}\right)$	$b = 4$	$\frac{\xi f_o}{u_{o_L}}$	28
$a = \frac{\pi}{2}\left(\frac{1}{.25}\right)$	$b = 2$	$\frac{\xi f_o}{u_{conv}}$	29
$c = 20$	$d = 100$	$\frac{\eta f_o}{u_{o_L}}$	30
$c = 10$	$d = 80$	$\frac{\eta f_o}{u_{conv}}$	31

It should be noted that these empirical expressions for the lateral and longitudinal correlation functions also satisfy the general requirements that

$$\psi_{f_o,R}(o,o,o) = 1$$

$$\lim_{\xi \to \infty} \psi_{f_o,R}(\xi,o,o) = 0$$

$$\lim_{\eta \to \infty} \psi_{f_o,R}(o,\eta,o) = 0$$

$$\left.\frac{\partial \psi_{f_o,R}(\xi,o,o)}{\partial \xi}\right|_{\xi = o} = \left.\frac{\partial \psi_{f_o,R}(o,\eta,o)}{\partial \eta}\right|_{\eta = o} = 0$$

$$\psi_{f_o,R}(\xi,o,o) = \psi_{f_o,R}(-\xi,o,o)$$

$$\psi_{f_o,R}(o,\eta,o) = \psi_{f_o,R}(o,-\eta,o) .$$

Estimates of the Longitudinal and Lateral Scales of Turbulence

The longitudinal space microscale is estimated from the time microscale and the convection velocity. This is accomplished by approximating the autocorrelation function with a parabola. The intersection of this parabola with the time delay axis determines a time delay, τ_o, which when multiplied by the appropriate convection velocity yields an estimate of the longitudinal scale.

In mathematical terms this relation is expressed as

$$\frac{1}{\lambda_\xi^2} \cong - \frac{1}{U_{conv}^2} \cdot \frac{1}{2} \left[\frac{\partial^2 \psi (o, o, \tau)}{\partial \tau^2} \right]_{\tau = 0}$$

which is obtained from approximating the auto-correlation function $\psi (o, o, \tau)$ with a Taylor series about the origin. The first two terms of the series, which yield a parabola, are used to approximate the function ψ for small values of time delays.

The estimates of longitudinal scale obtained over the various broad-frequency bands are plotted in Fig 32 as a function of Reynolds number. The average value of the longitudinal scale λ_ξ is approximately 0.15 inches.

Estimates of the longitudinal scale were also obtained by the same method for the various octave frequency bands investigated at each Reynolds number. These data are presented as functions of frequency (geometric mean center frequency) for the various Reynolds numbers in Fig. 33. As expected, the scale becomes smaller as the frequency increases. A definite Reynolds number dependence, which can not be explained by experimental error alone, is exhibited by the measurements of longitudinal scale in octave bands.

Estimates of the longitudinal scale in octave frequency bands were also obtained from the longitudinal correlation coefficient data as represented by the empirical expression shown in Fig. 29 as a function of Strouhal number based on convection velocity. Letting S_ξ be a measure of the distance between the origin and the point of intersection on the Strouhal number axis of the osculation parabola at the vertex of the correlation curve, the following relation is obtained:

$$- \frac{2}{S_\xi^2} = \left. \frac{\partial^2 \psi_{t_o, R} (\xi, o, o)}{\partial S^2} \right|_{S = 0} = -a^2 - 2b$$

where

$$S_\xi = \frac{\lambda_\xi f_o}{u_{conv}}$$

and a and b are the constants used in fitting the empirical relation to the data of Fig. 29. For the case at hand, $a = 2\pi$ and $b = 2$, yielding

$$S_\xi^2 = \left(\frac{\lambda_\xi f_o}{u_{conv}}\right)^2 = \frac{2}{4\pi^2 + 4}$$

or

$$\lambda_\xi = 0.214 \frac{u_{conv}}{f_o} .$$

The values of λ_ξ determined from the above relation based on the Strouhal number representation of the data are plotted versus frequency for the various Reynolds numbers in Fig. 34.

A comparison of Fig. 33 with Fig. 34 indicates very close agreement between the two methods of estimating the longitudinal scale in octave frequency bands.

A similar treatment of the lateral correlation coefficient data shown in Fig. 31 as a function of Strouhal number based on convection velocity yields the following relation:

$$-\frac{2}{S_\eta^2} = \left.\frac{\partial^2 \psi_{f_o,R}(o,\eta,o)}{\partial S^2}\right|_{s=0} = -2(c+d)$$

where

$$S_\eta = \frac{\lambda_\eta f_o}{u_{conv}}$$

and the determined values of the constants are $c = 10$ and $d = 80$. Substitution of these values yields

$$\lambda_\eta = 0.105 \frac{u_{conv}}{f_o} .$$

The values of λ_η determined from the above relation are shown in Fig. 35 as a function of frequency for the various Reynolds numbers investigated.

A comparison of the estimates of longitudinal and lateral scales obtained from the correlation data as functions of Strouhal number indicates that for any given octave frequency band at a specified Reynolds number

$$\frac{\lambda_\eta}{\lambda_\xi} = \frac{0.105}{0.214}$$

or

$$\lambda_\eta = 0.49\,\lambda_\xi$$

On the basis of this information for octave frequency bands, it has been assumed that the broad-band scales are similarly related. Thus, in all the correction factors on a broad-band basis the lateral scale has been taken as half of the longitudinal scale. (It should be noted that if the lateral scale were actually larger than half of the longitudinal scale, the necessary corrections for transducer size to the root-mean-square pressure and the frequency spectra would become even smaller than those used in this report.)

SUMMARY AND CONCLUSION

Broad-band measurements of the pressure fluctuations are similar to those reported by other investigators of the turbulent boundary layer. The ratio of the corrected root-mean-square pressure to the dynamic pressure lies within the range of 0.0062 to 0.0049. The broad-band pressure field at the wall is convected downstream at approximately 0.70 of the centerline velocity over the range of Reynolds numbers from 100,000 to 300,000. Estimates of the scales of the turbulence indicate that the lateral scale is of the order of half of the longitudinal scale.

The more important aspect of the current investigation is the emphasis on the octave frequency band measurements. Convection velocity data in octave frequency bands indicate a definite frequency dependence with the ratio of convection velocity to centerline velocity varying from approximately unity at the low frequencies to 0.64 at the high frequencies. No dependence of this ratio on Reynolds number is detectable.

Space-time correlations in octave bands indicate that the correlation maxima of the high-frequency components of the pressure field at the wall decay at a

substantially faster rate than the correlation maxima of the low-frequency components. Longitudinal correlations plotted versus Strouhal number show that the data obtained at various transducer separations, frequencies, and Reynolds numbers define a single function. Lateral correlation data also define a single function of Strouhal number. (These functions are of distinctly different types, as is readily evident from the data and from the fitted curves.)

Finally, estimates of the scales of the turbulence within octave frequency bands indicate that the lateral scale is approximately half of the longitudinal scale within any specified frequency band.

Since other experimental studies of the turbulent boundary layer have not concentrated on the frequency-dependent characteristics of the measured quantities, few comparisons can be made. However, because of the reliability of the instrumentation, the consistent repeatability of these data, and the small size of the transducers used in the present investigations, it is believed that these data represent a further step in the direction of an understanding of the turbulent processes.

In conclusion, further investigations are in progress in the turbulent flow facility at the Underwater Sound Laboratory. These investigations are to be carried out over a wider range of transducer separations and in narrower frequency bands. Also an attempt will be made to investigate static pressure fluctuations within the flow and the relation between pressure and velocity fluctuations.

na

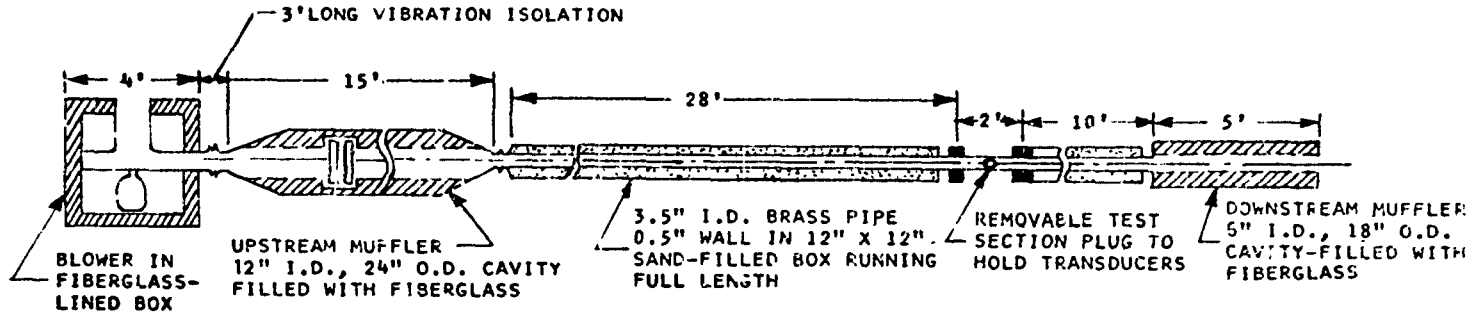

Fig. 1 - Diagram of the Turbulent Pipe Flow Facility

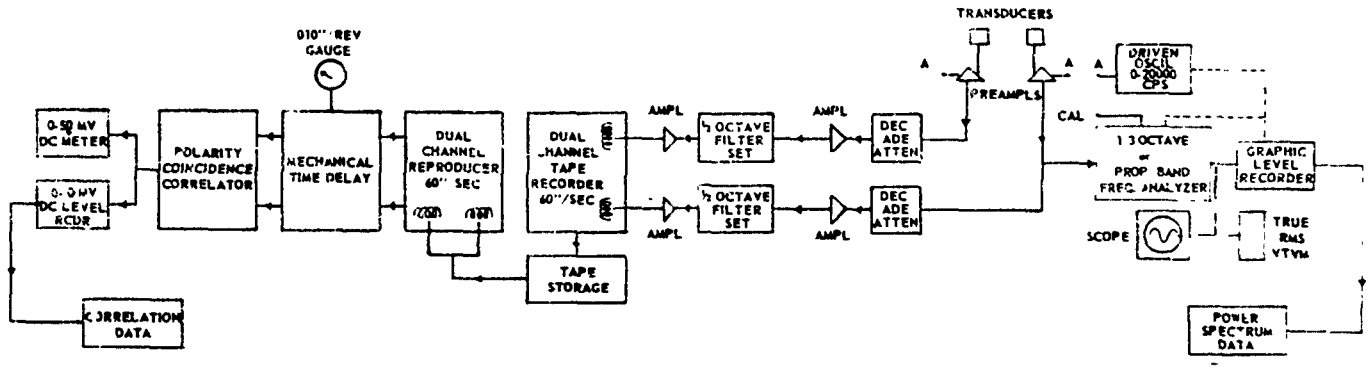

Fig. 2 - Block Diagram of Instrumentation System

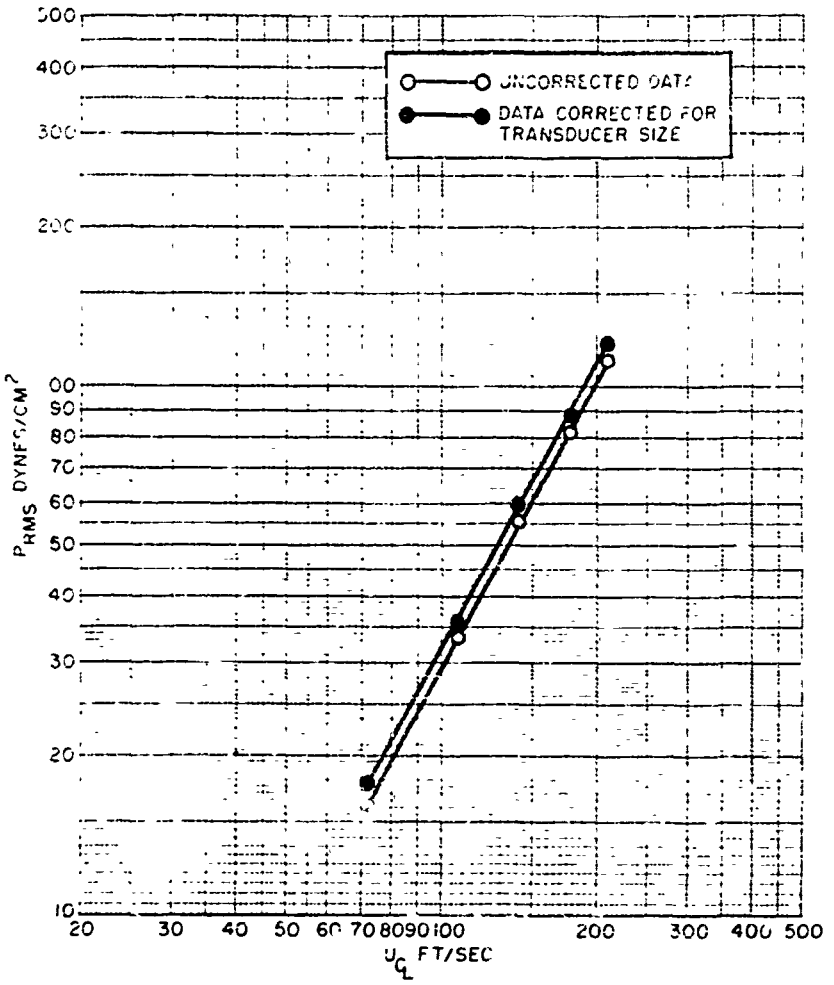

Fig. 3 - Root-Mean-Square Pressure versus Centerline Velocity

7

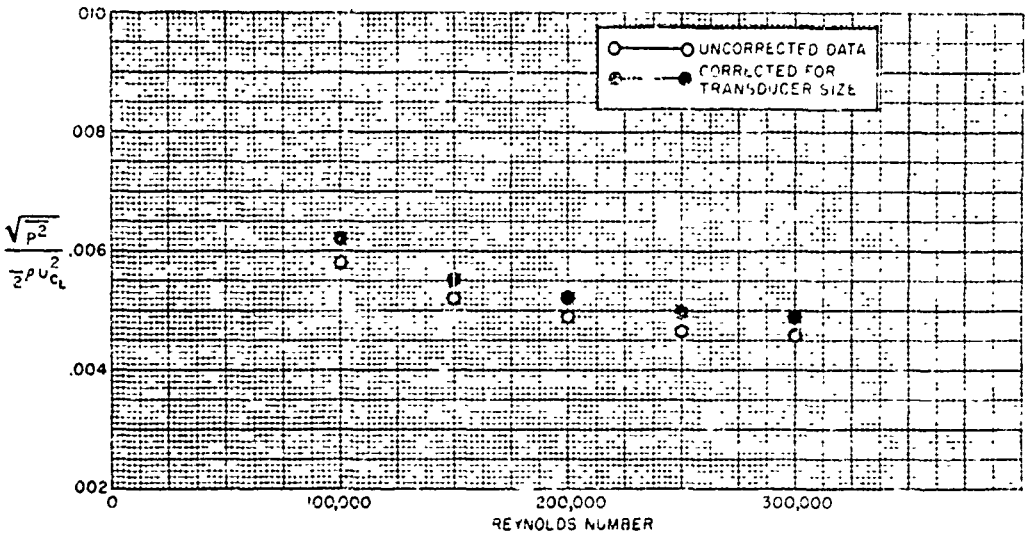

Fig. 4 - Root-Mean-Square Pressure Coefficient versus Reynolds Number

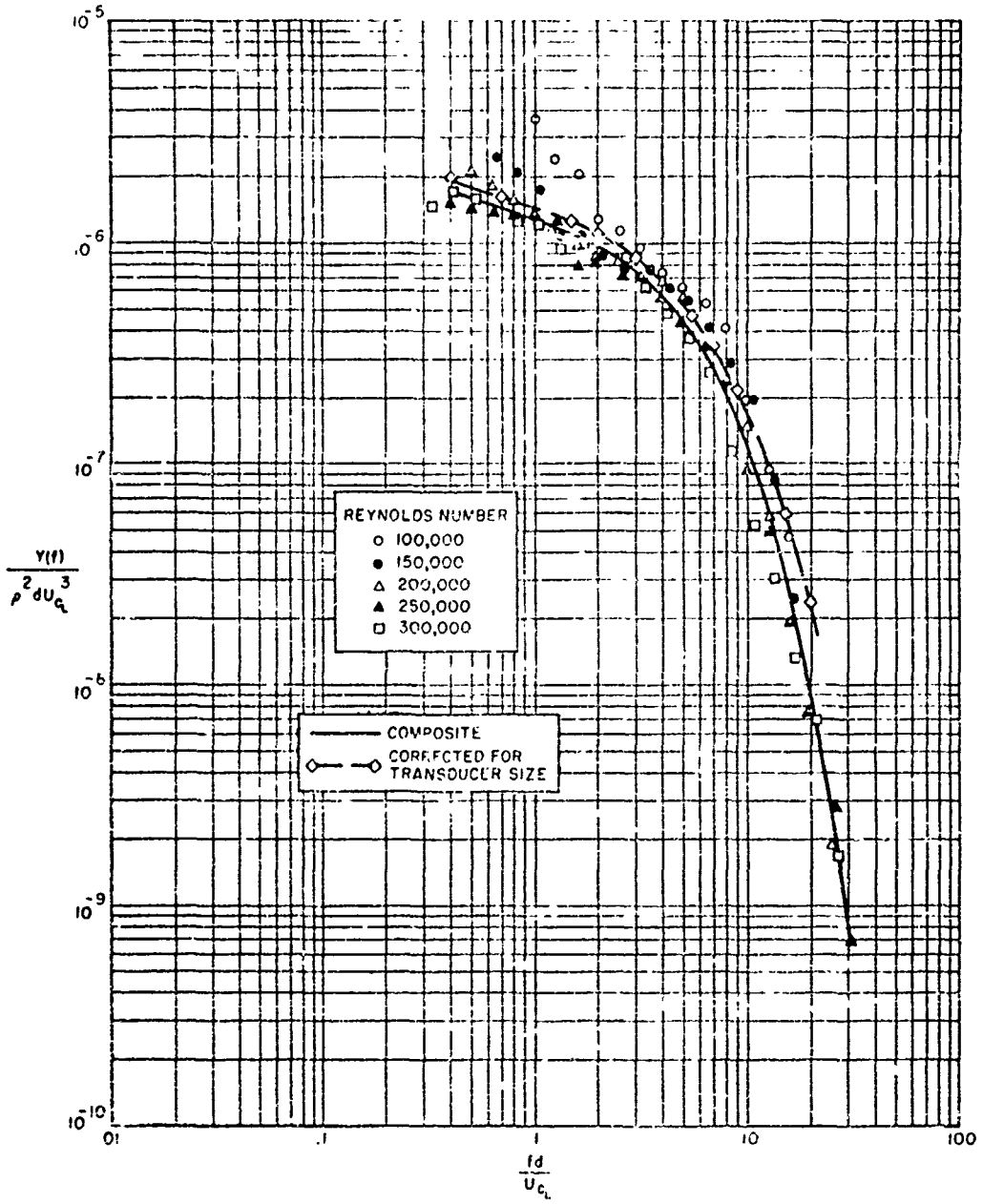

Fig. 5 - The Non-Dimensionalized Frequency Spectrum

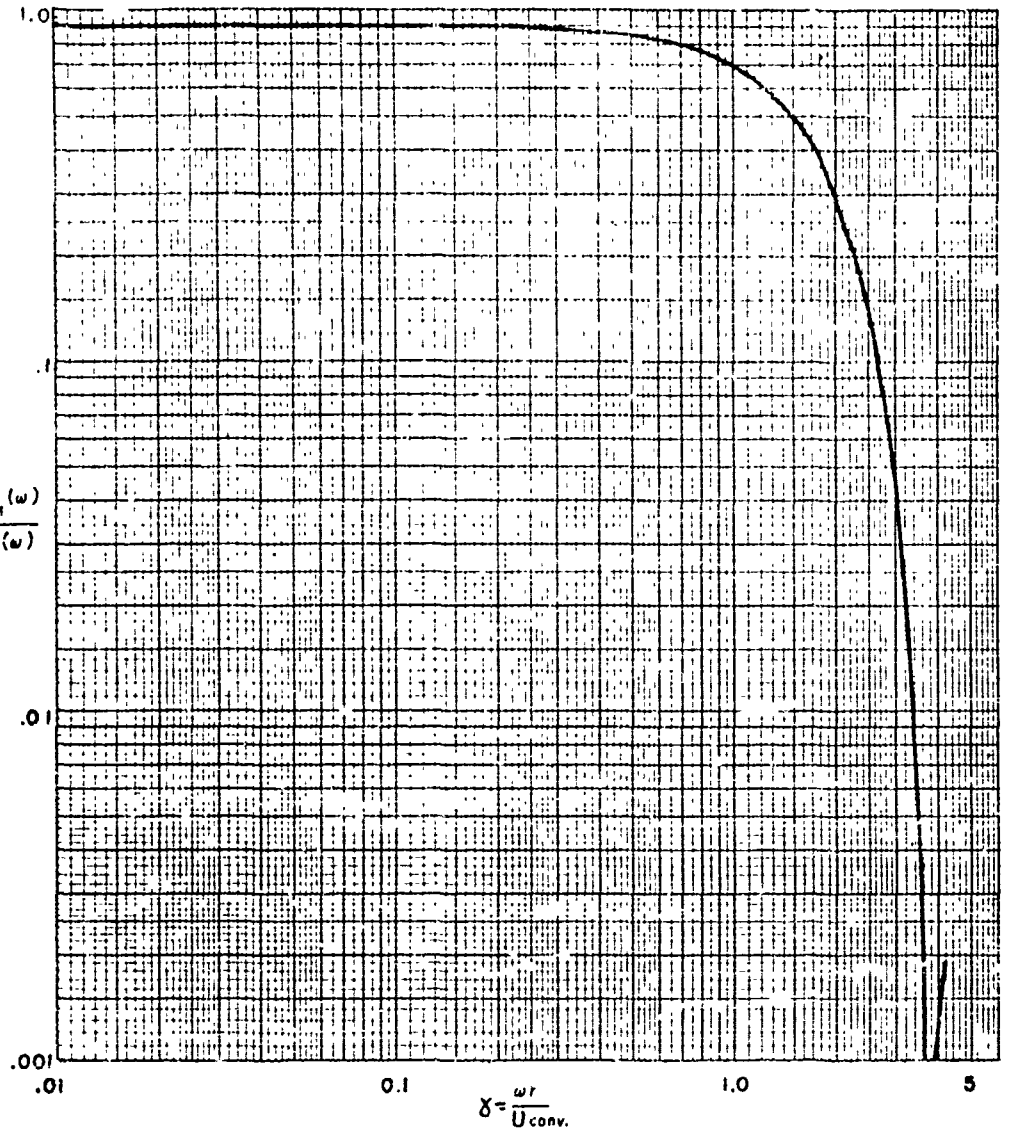

Fig. 6 - Correction to Power Density for Finite Transducer Size

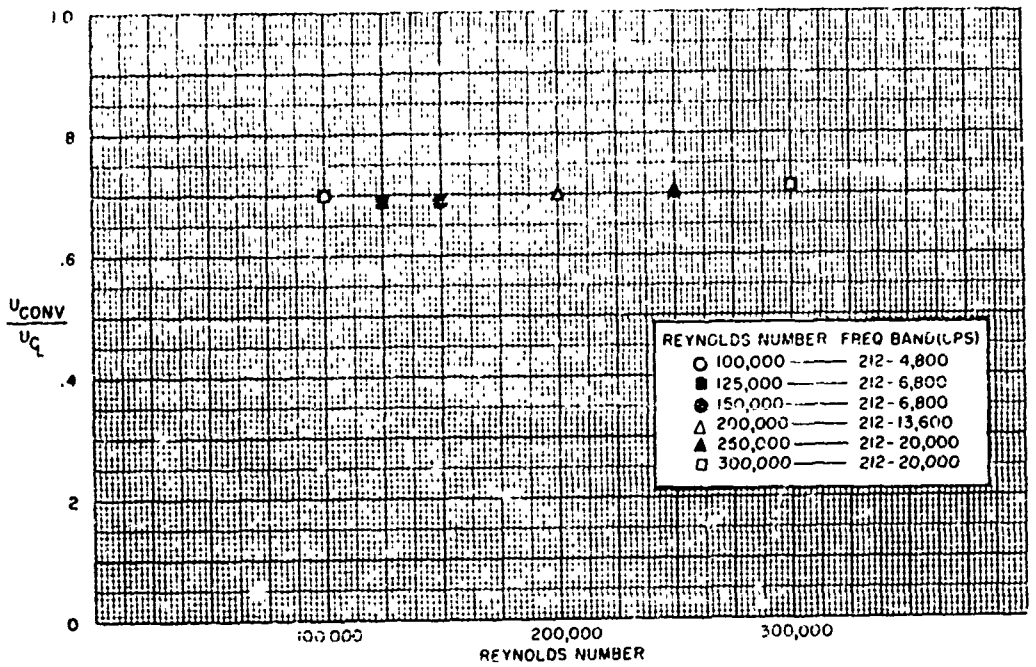

Fig. 7 - Ratio of Convection Velocity to Centerline Velocity versus Reynolds Number

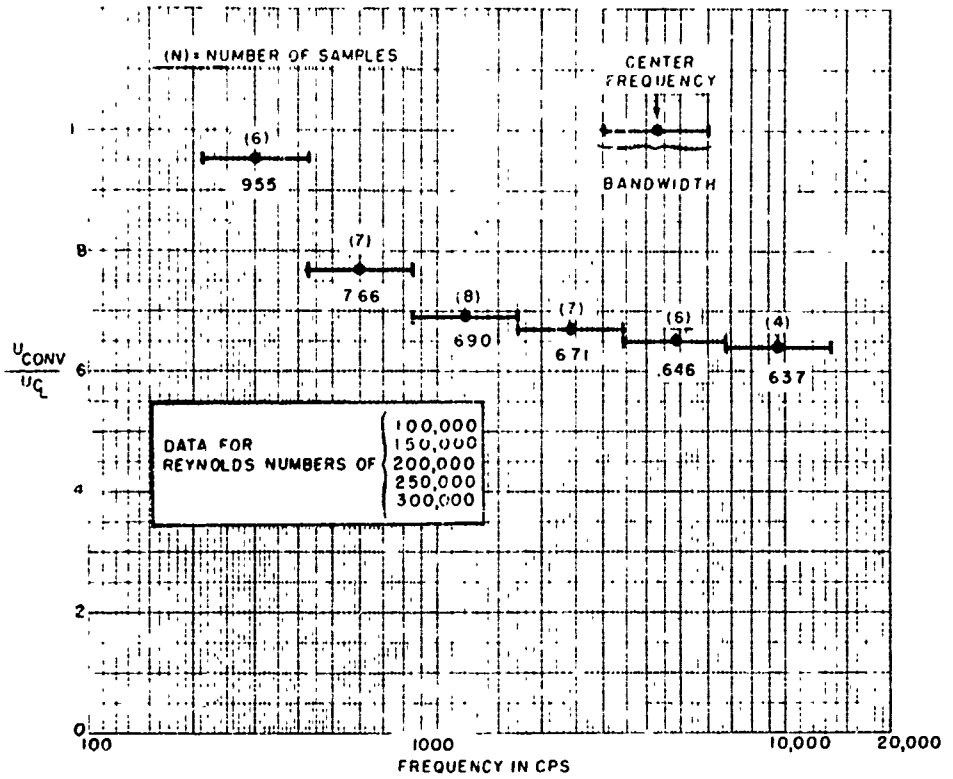

Fig. 8 - Ratio of Convection Velocity to Centerline Velocity versus Frequency

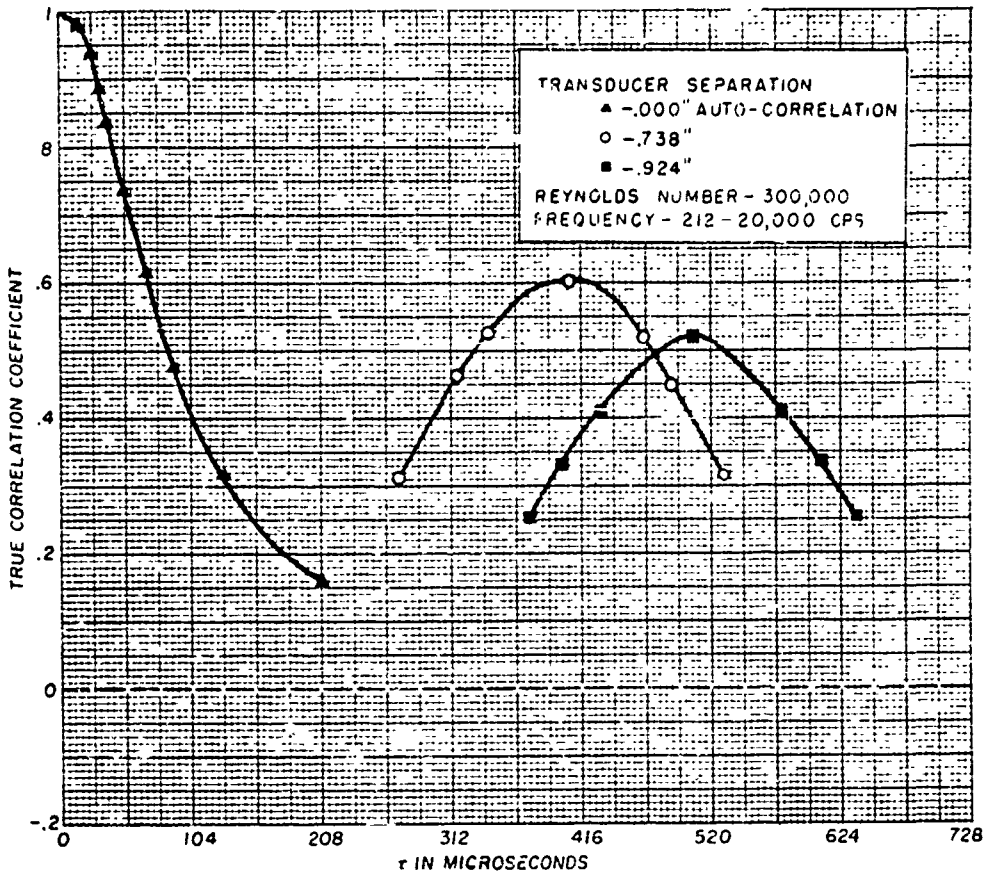

Fig. 9 - Cross-Correlation versus Time Delay for the Frequency Band 212-20,000 cps

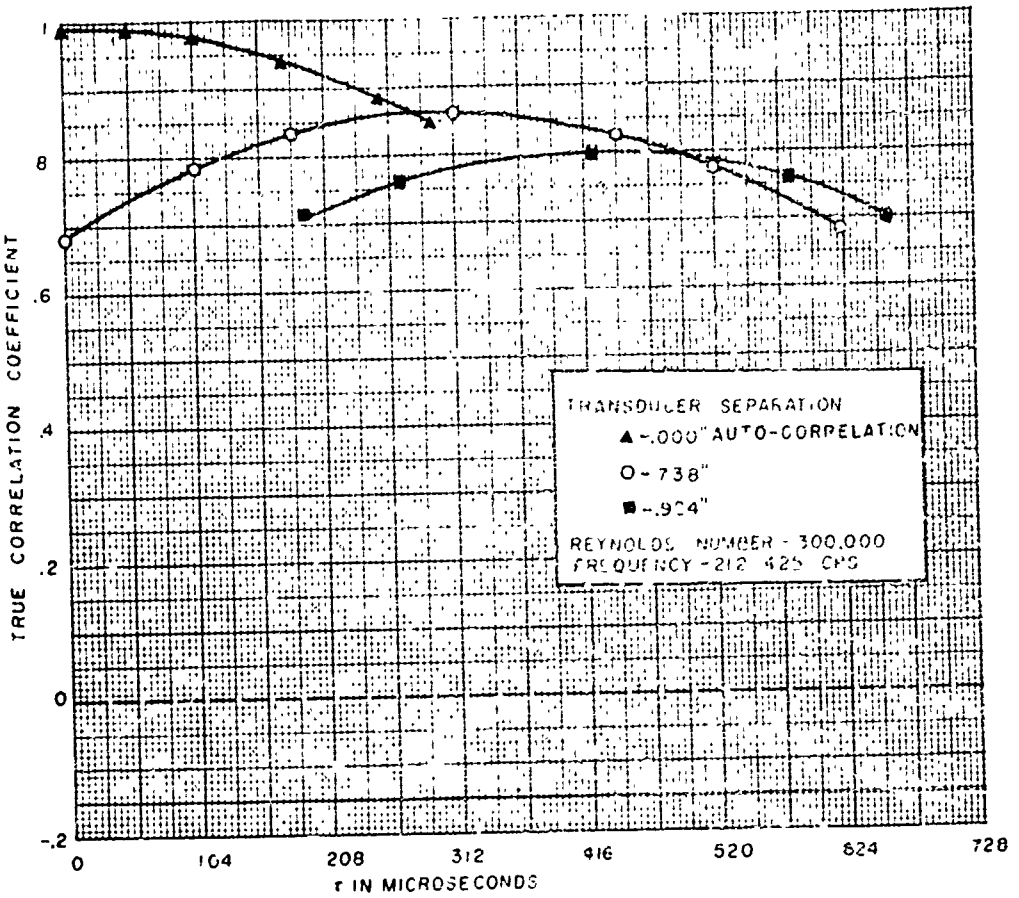

Fig. 10 - Cross-Correlation versus Time Delay for the Frequency Band 212-425 cps

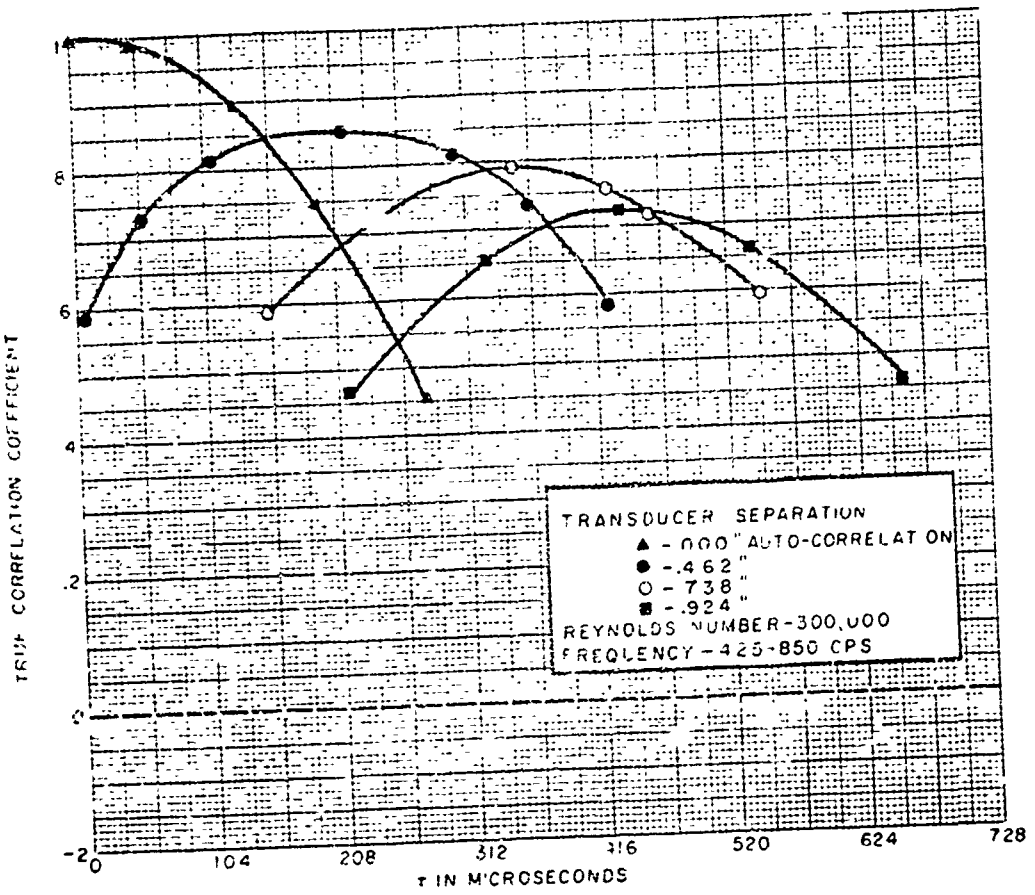

Fig. 11 - Cross-Correlation versus Time Delay for the Frequency Band 425-850 cps

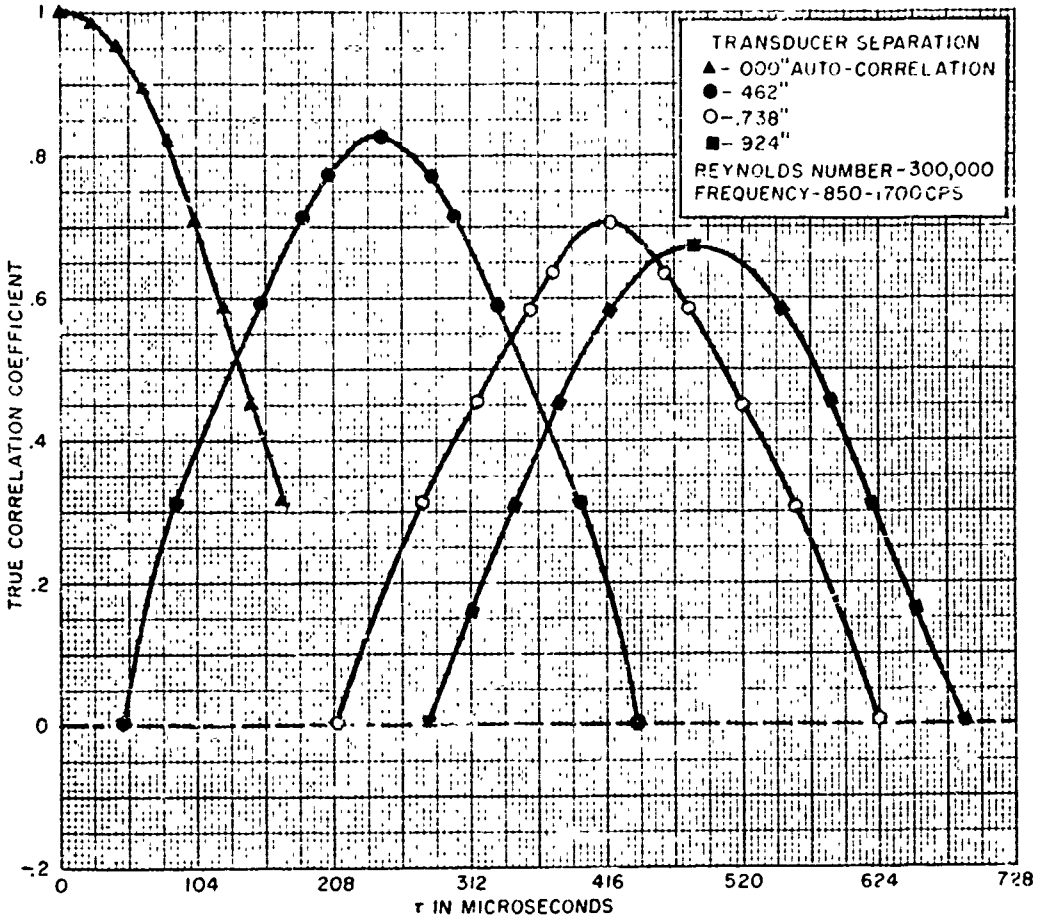

Fig. 12 - Cross-Correlation versus Time Delay for the Frequency Band 850-1700 cps

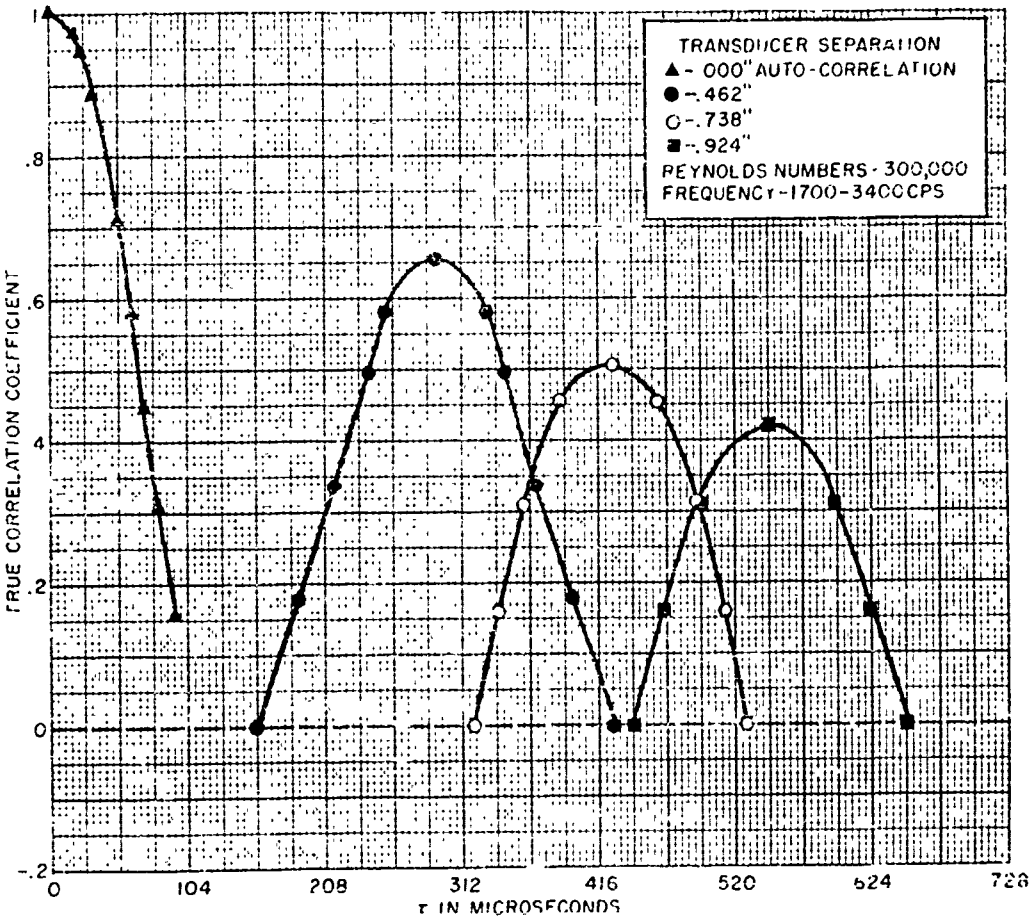

Fig. 13 - Cross-Correlation versus Time Delay for the Frequency Band 1700-3400 cps

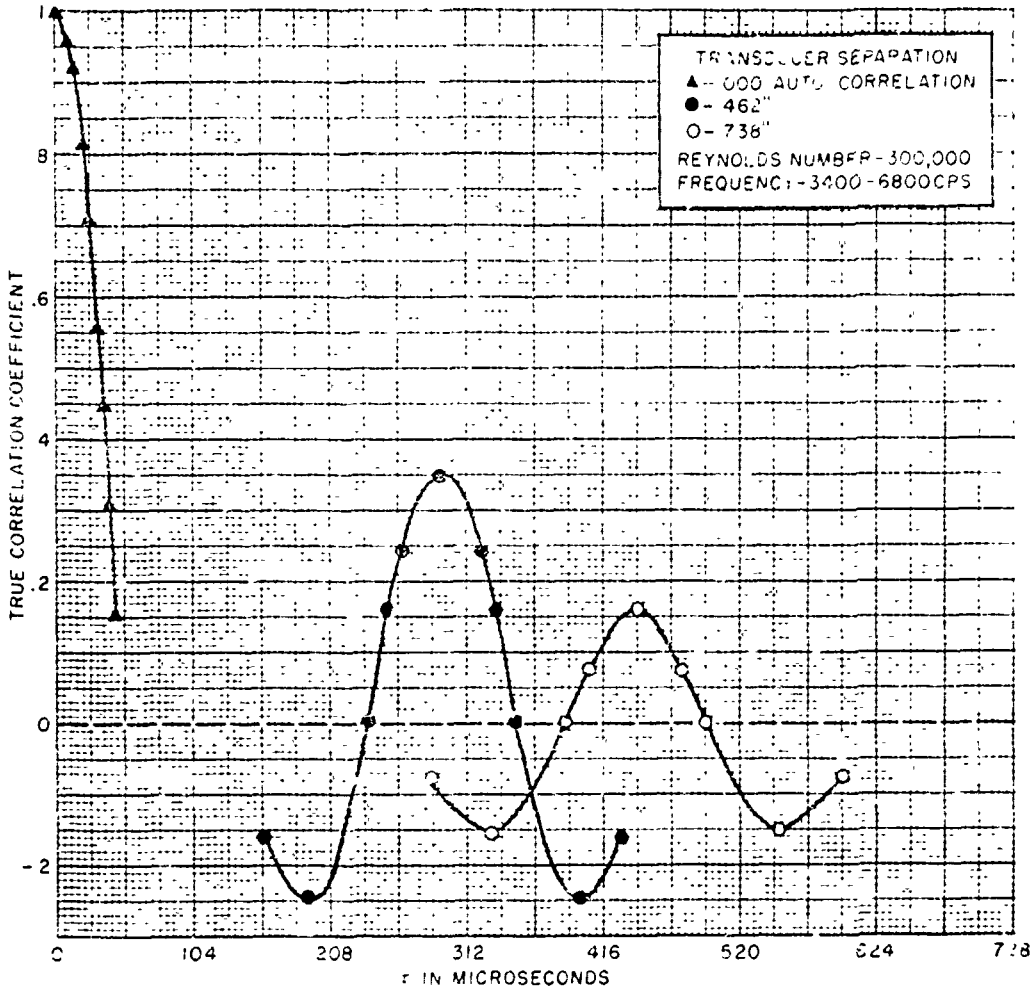

Fig. 14 - Cross-Correlation versus Time Delay for the Frequency Band 3400-6800 cps

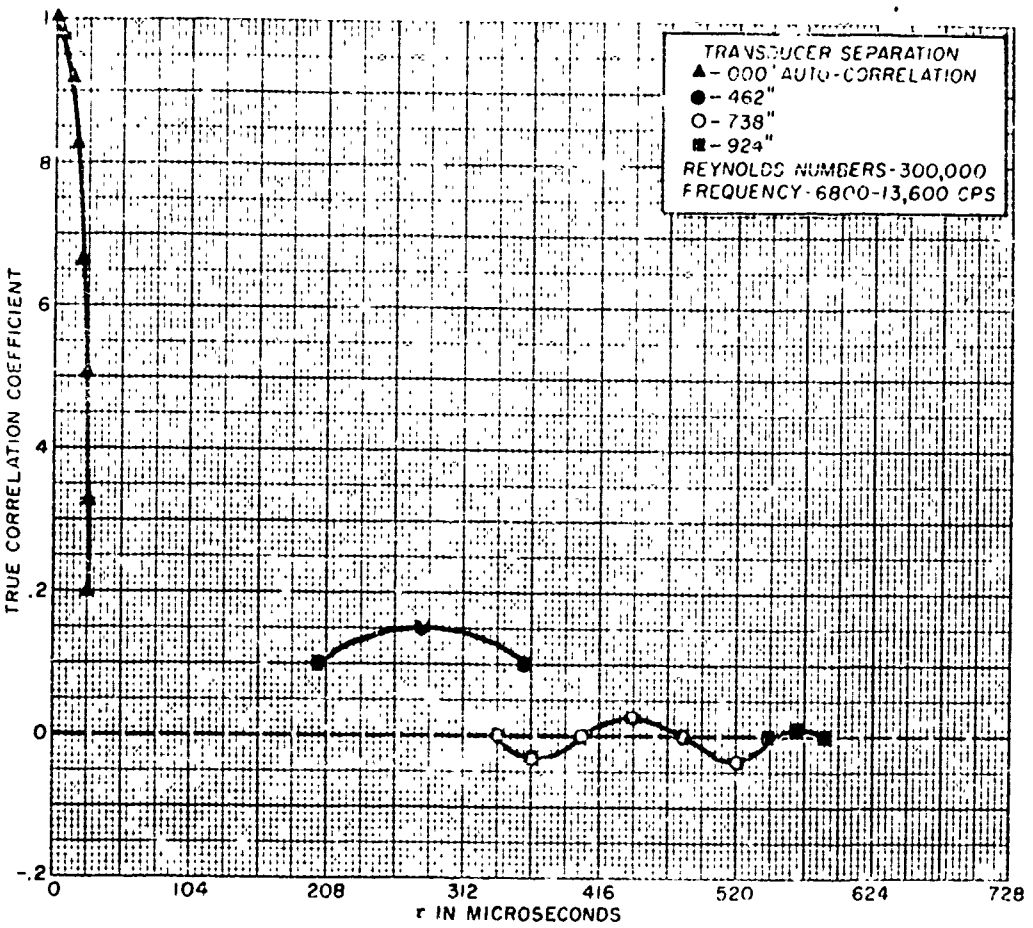

Fig. 15 - Cross-Correlation versus Time Delay for the Frequency Band 6800-13,600 cps

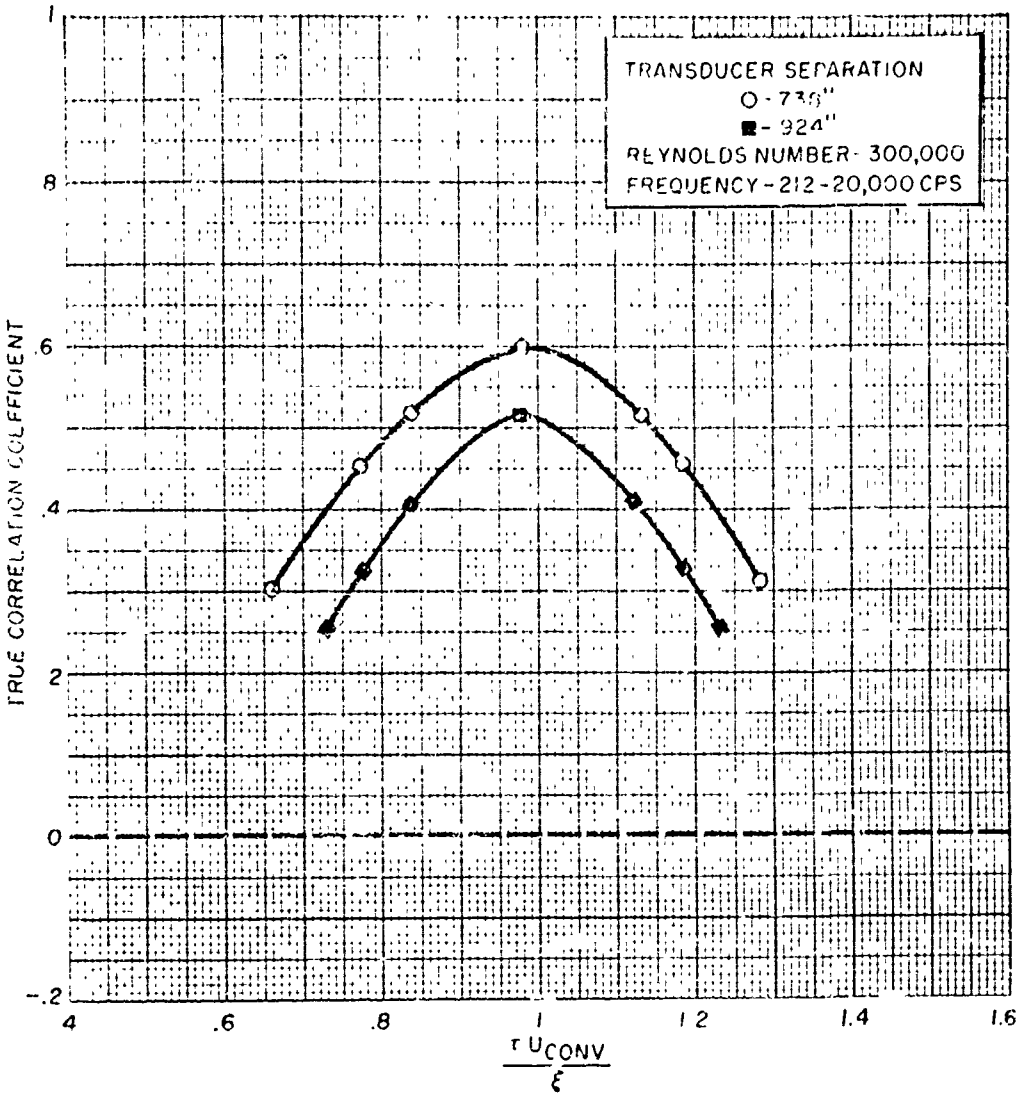

Fig. 16 - Cross-Correlation versus Non-Dimensional Time Delay for the Frequency Band 212-20,000 cps

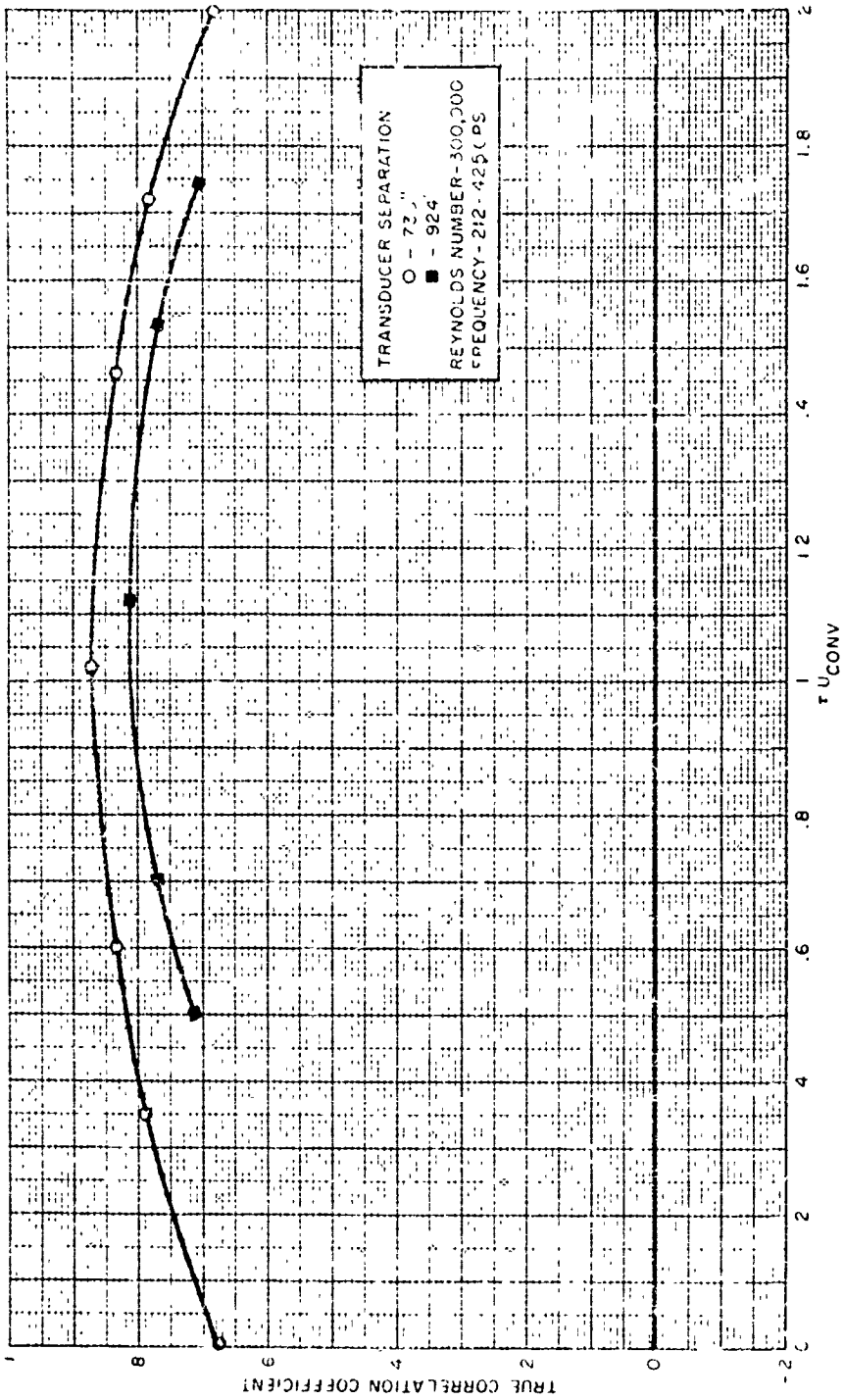

Fig. 17 - Cross-Correlation versus Non-Dimensional Time Delay for the Frequency Band 212-425 cps

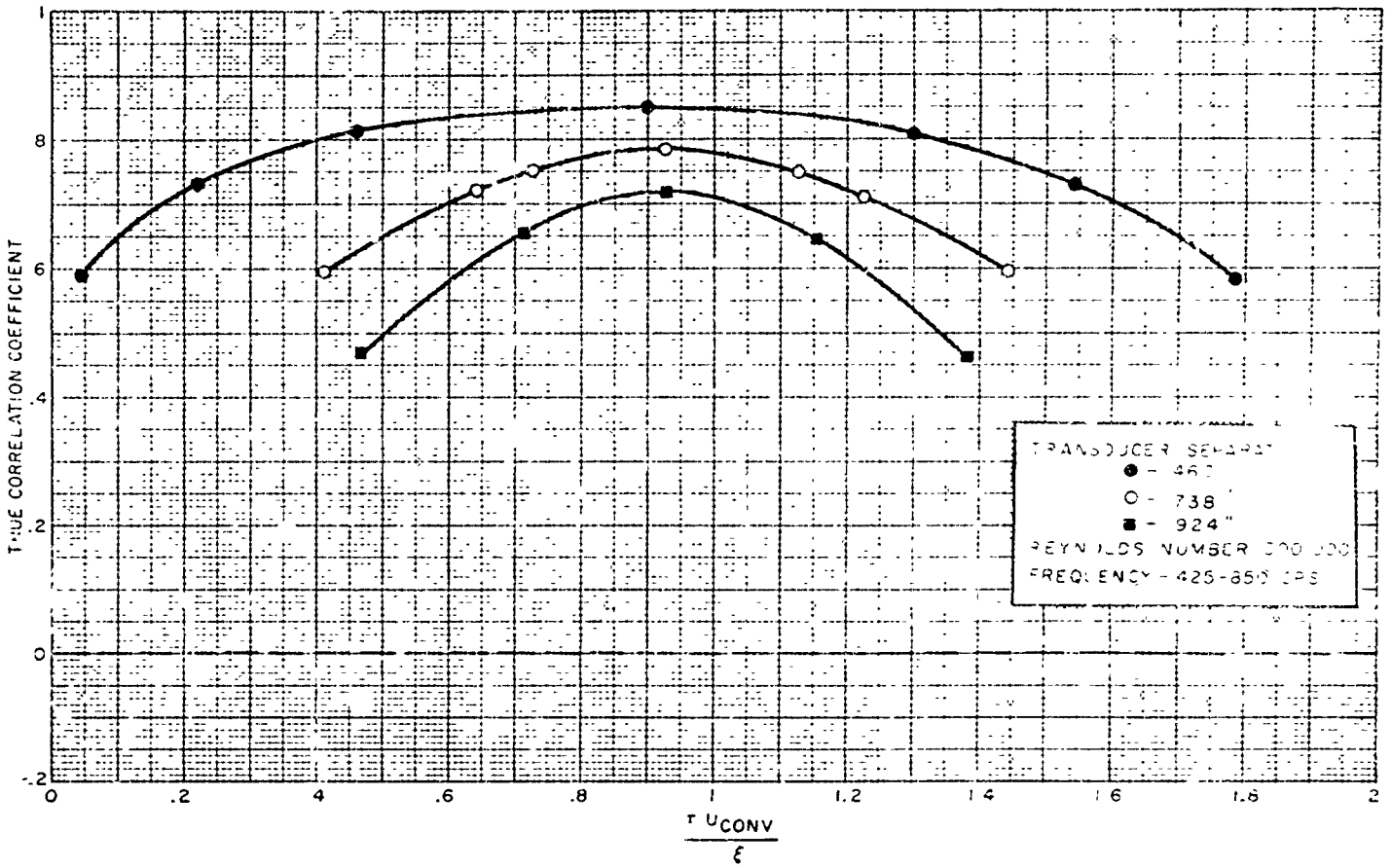

Fig. 18 - Cross-Correlation versus Non-Dimensional Time Delay for the Frequency Band 425-850 cps

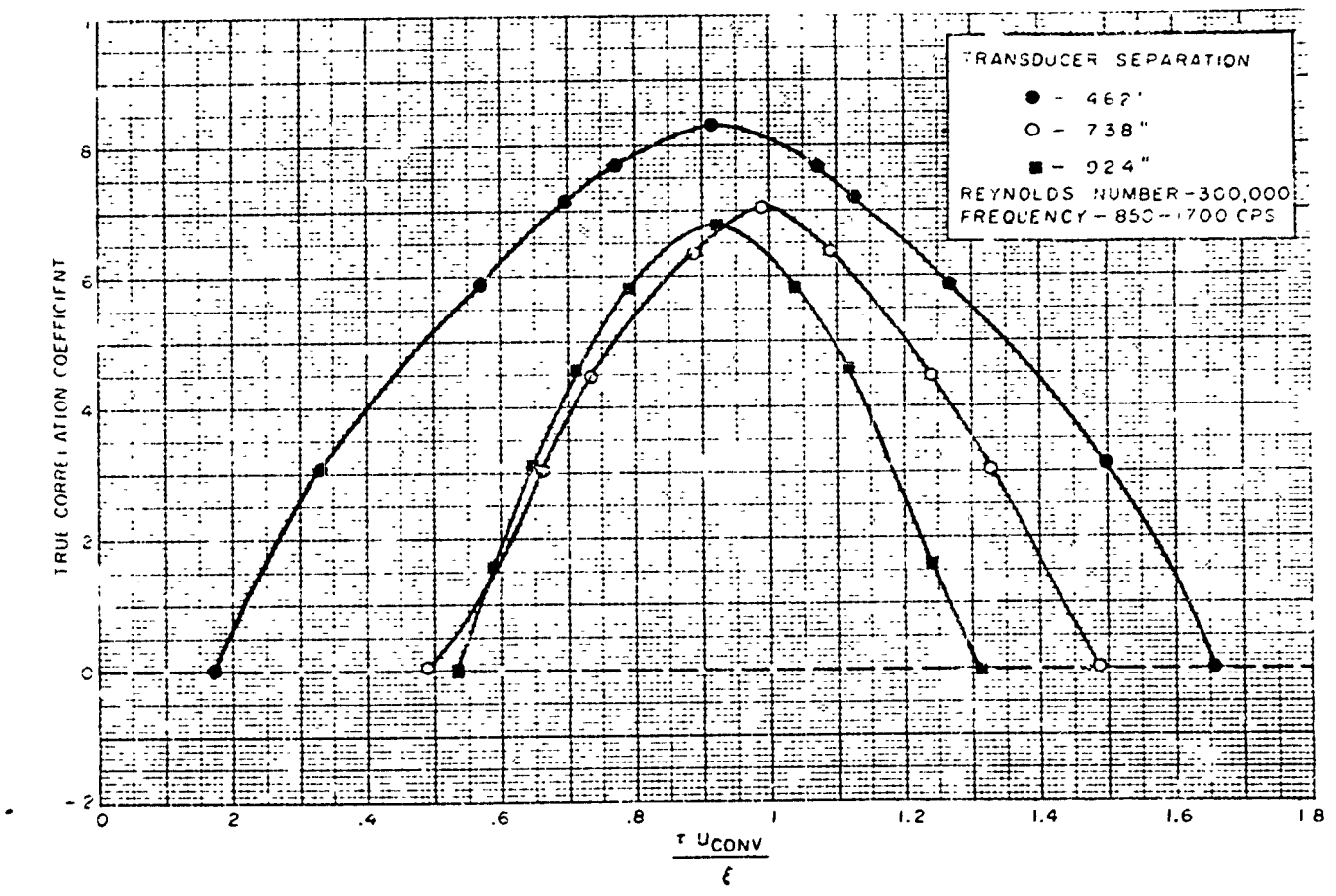

Fig. 19 - Cross-Correlation versus Non-Dimensional Time Delay for the Frequency Band 850-1700 cps

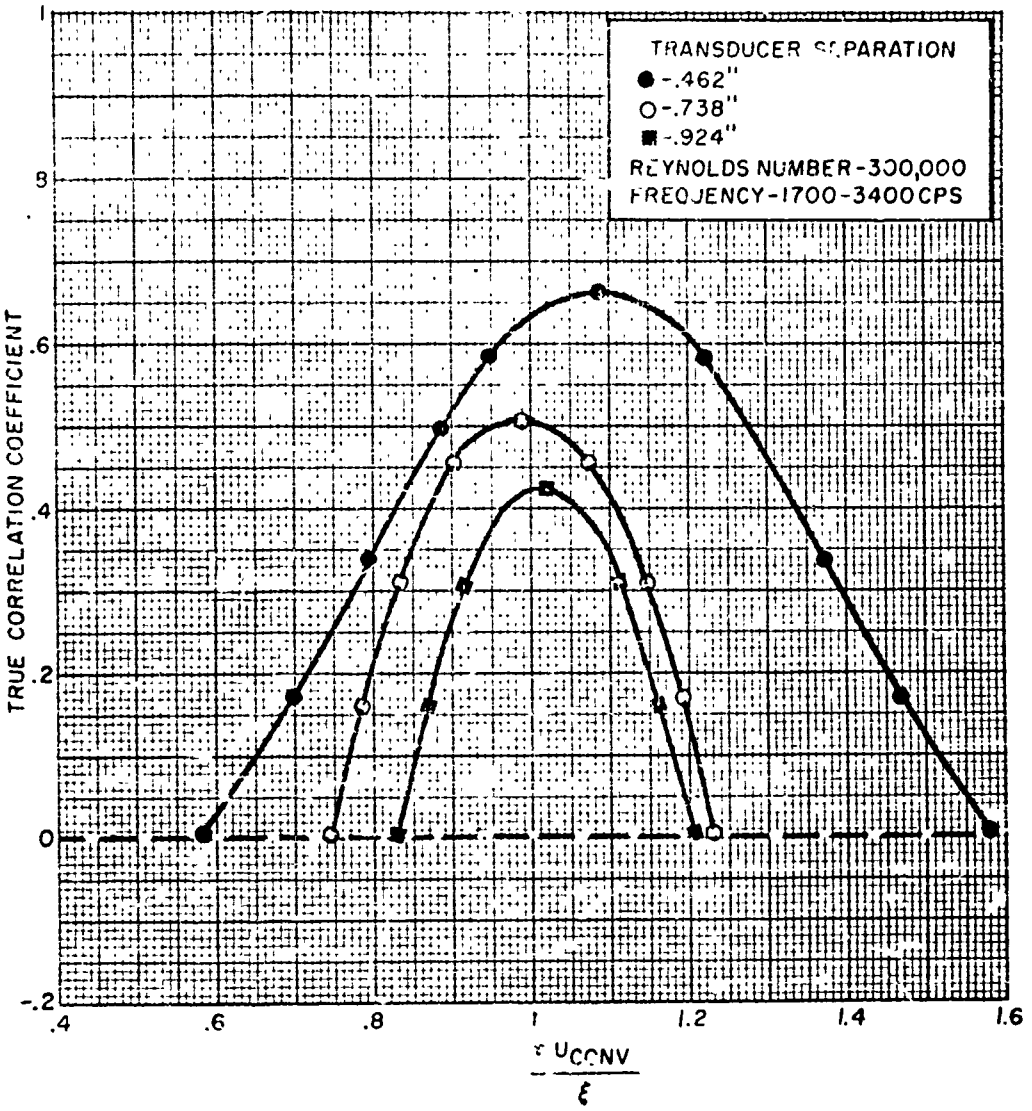

Fig. 20 - Cross-Correlation versus Non-Dimensional Time Delay for the Frequency Band 1700-3400 cps

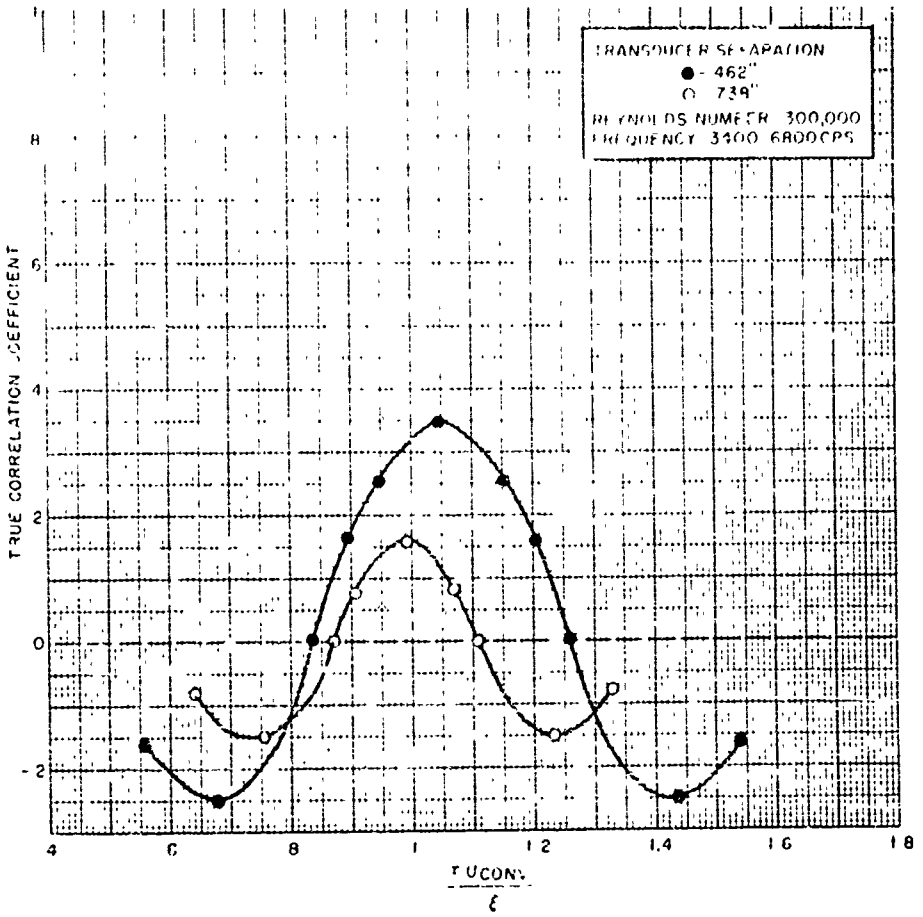

Fig. 21 - Cross-Correlation versus Non-Dimensional Time Delay for the Frequency Band 3400-6800 cps

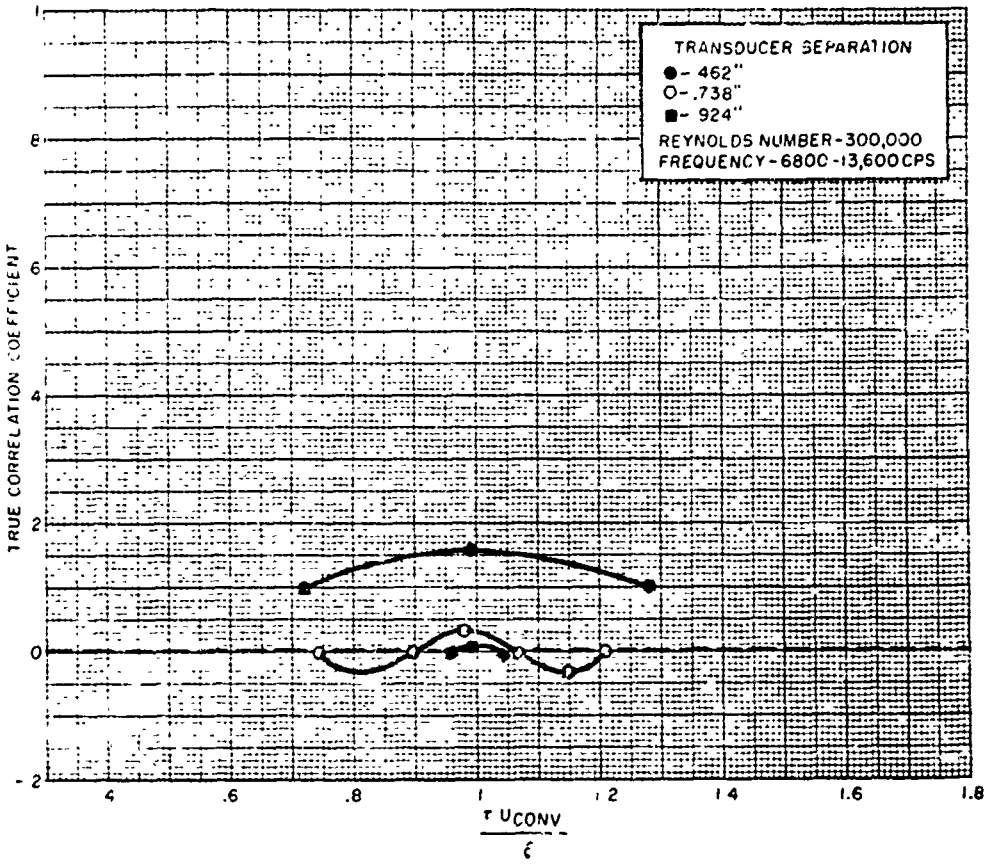

Fig. 22 - Cross-Correlation versus Non-Dimensional Time Delay for the Frequency Band 6800-13,600 cps

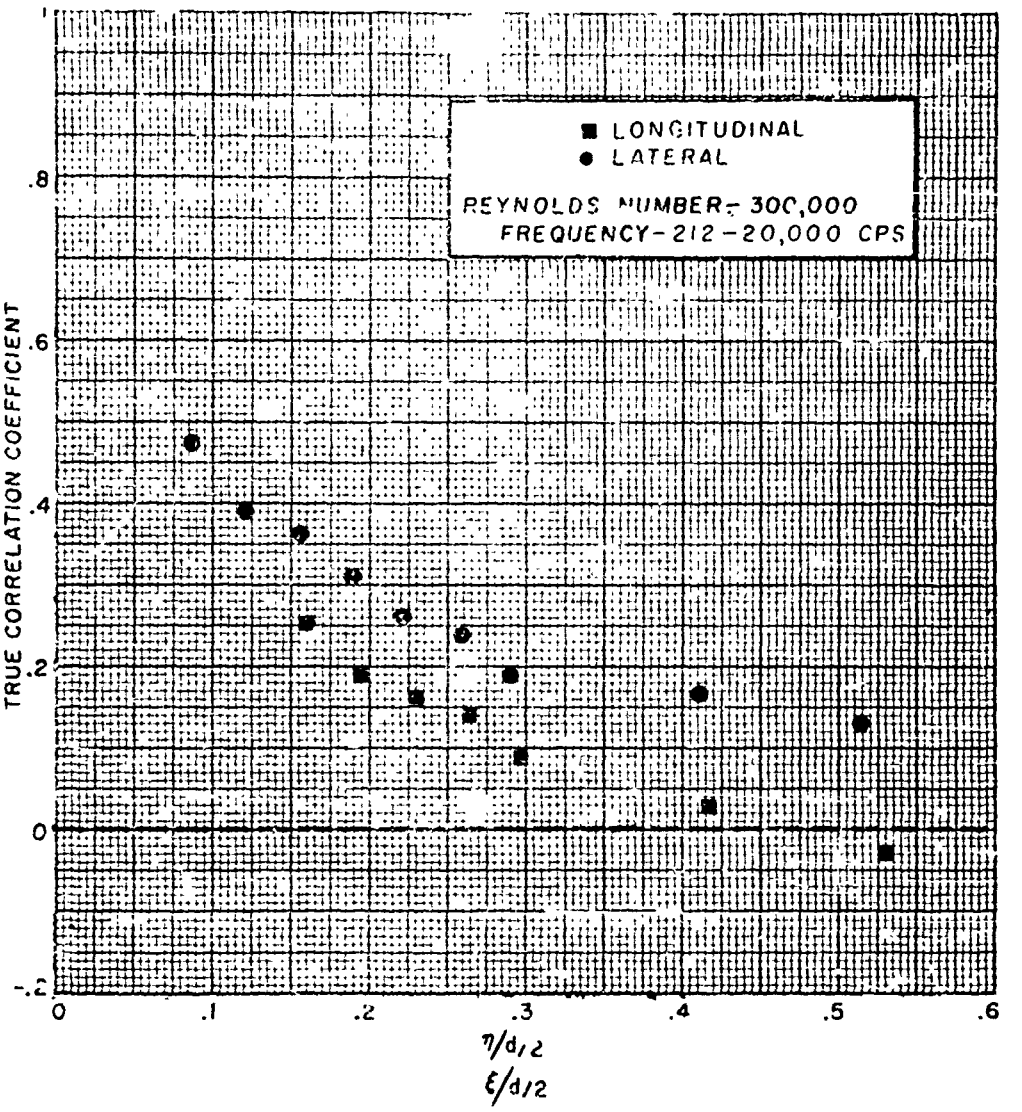

Fig. 23 - Space Correlation at a Reynolds Number of 800,000

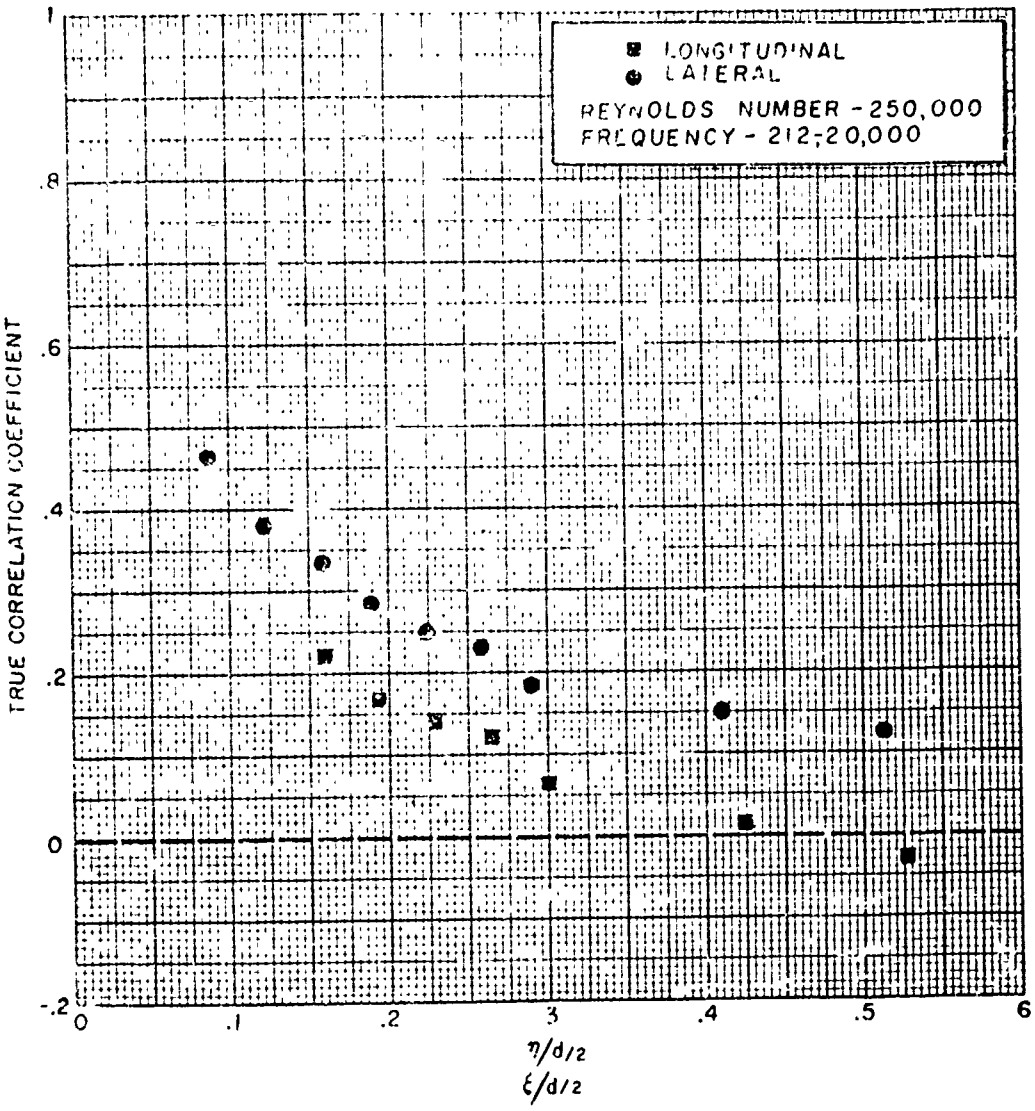

Fig. 24 - Space Correlation at a Reynolds Number of 250,000

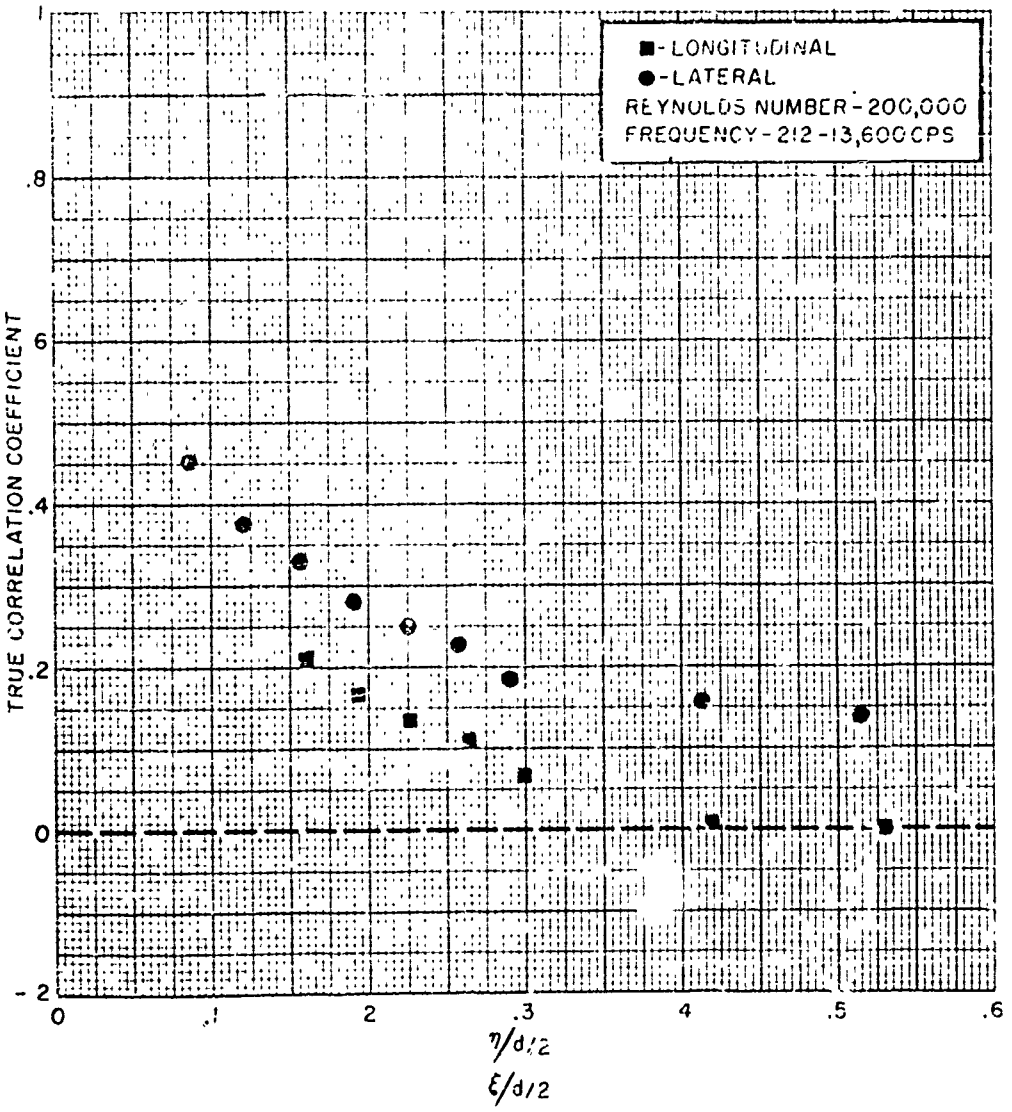

Fig. 25 - Space Correlation at a Reynolds Number of 200,000

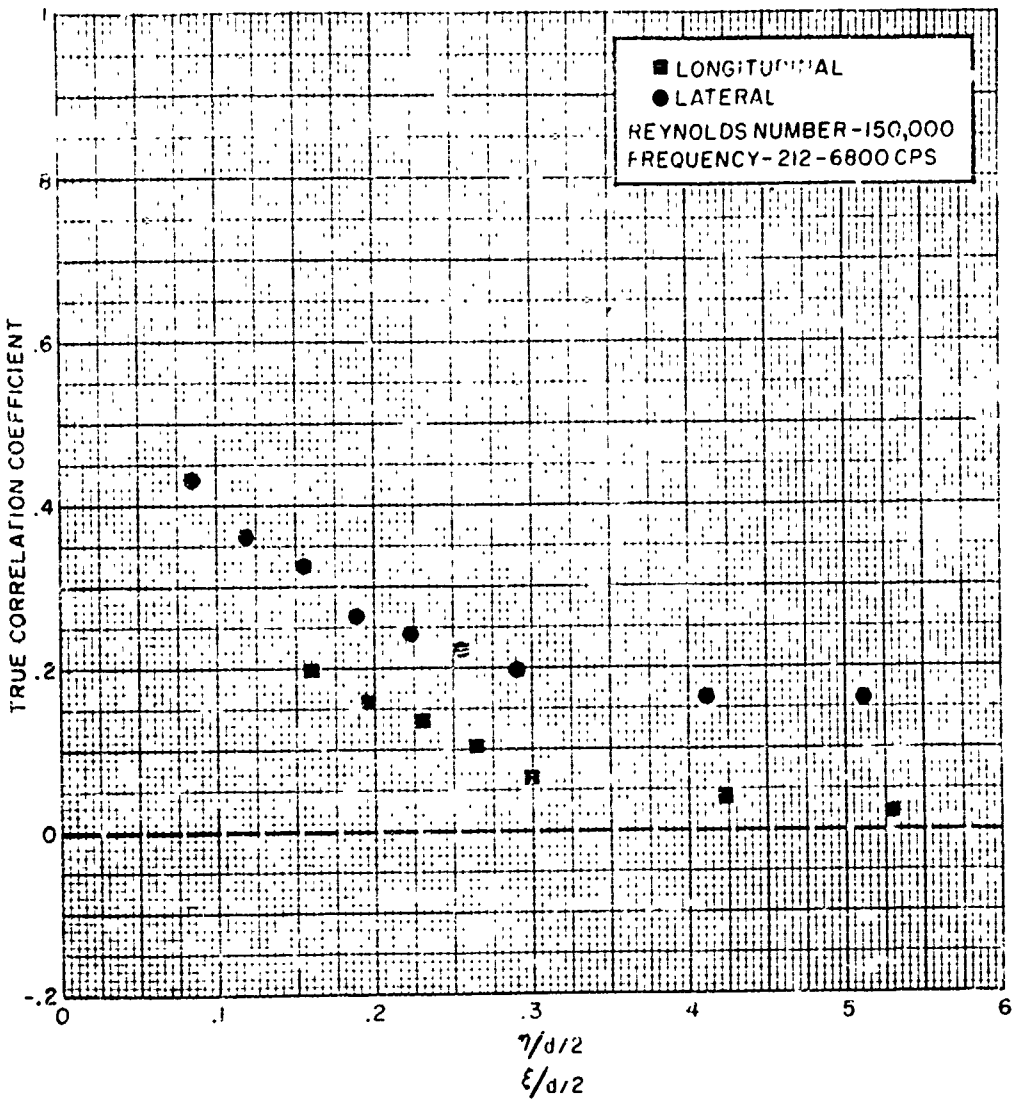

Fig. 26 - Space Correlation at a Reynolds Number of 150,000

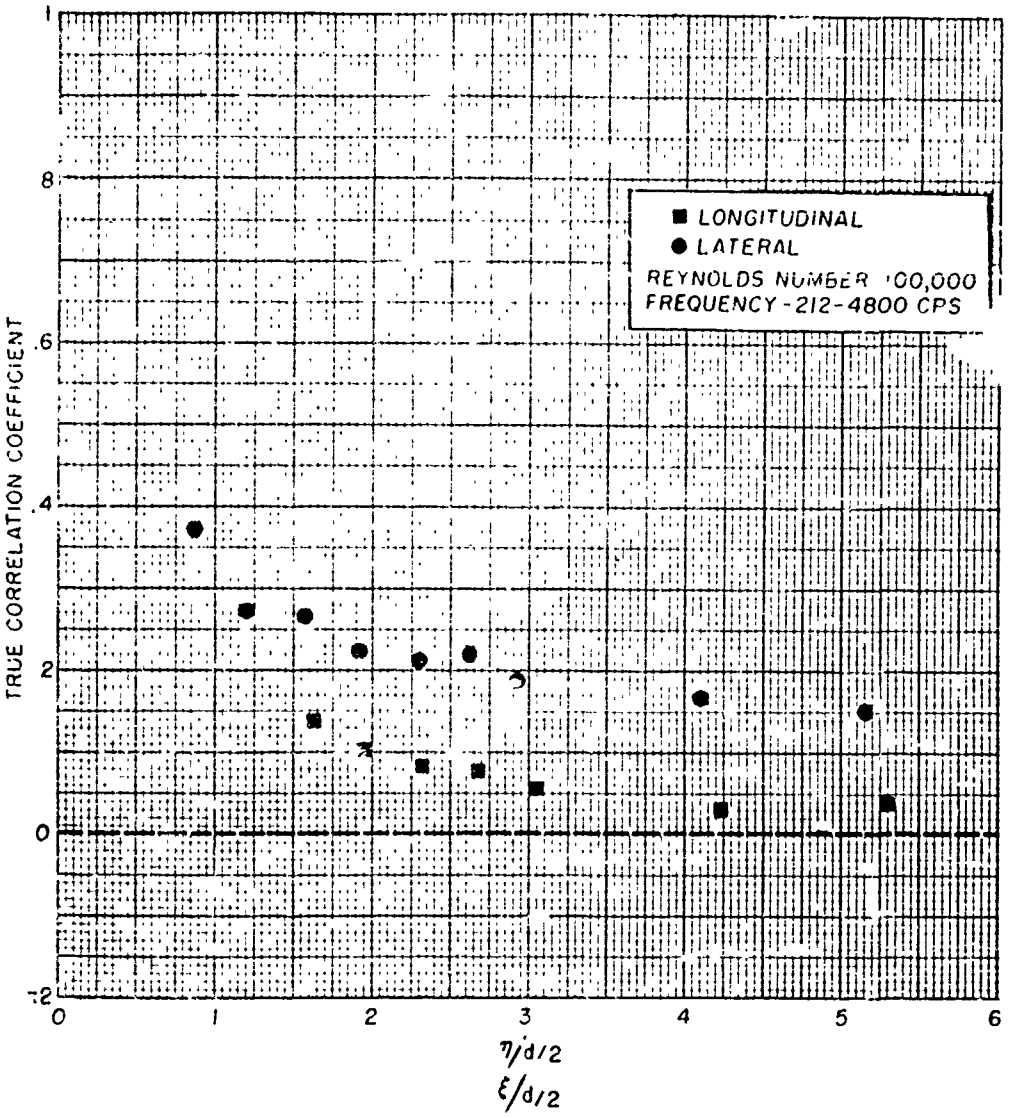

Fig. 27 - Space Correlation at a Reynolds Number of 100,000

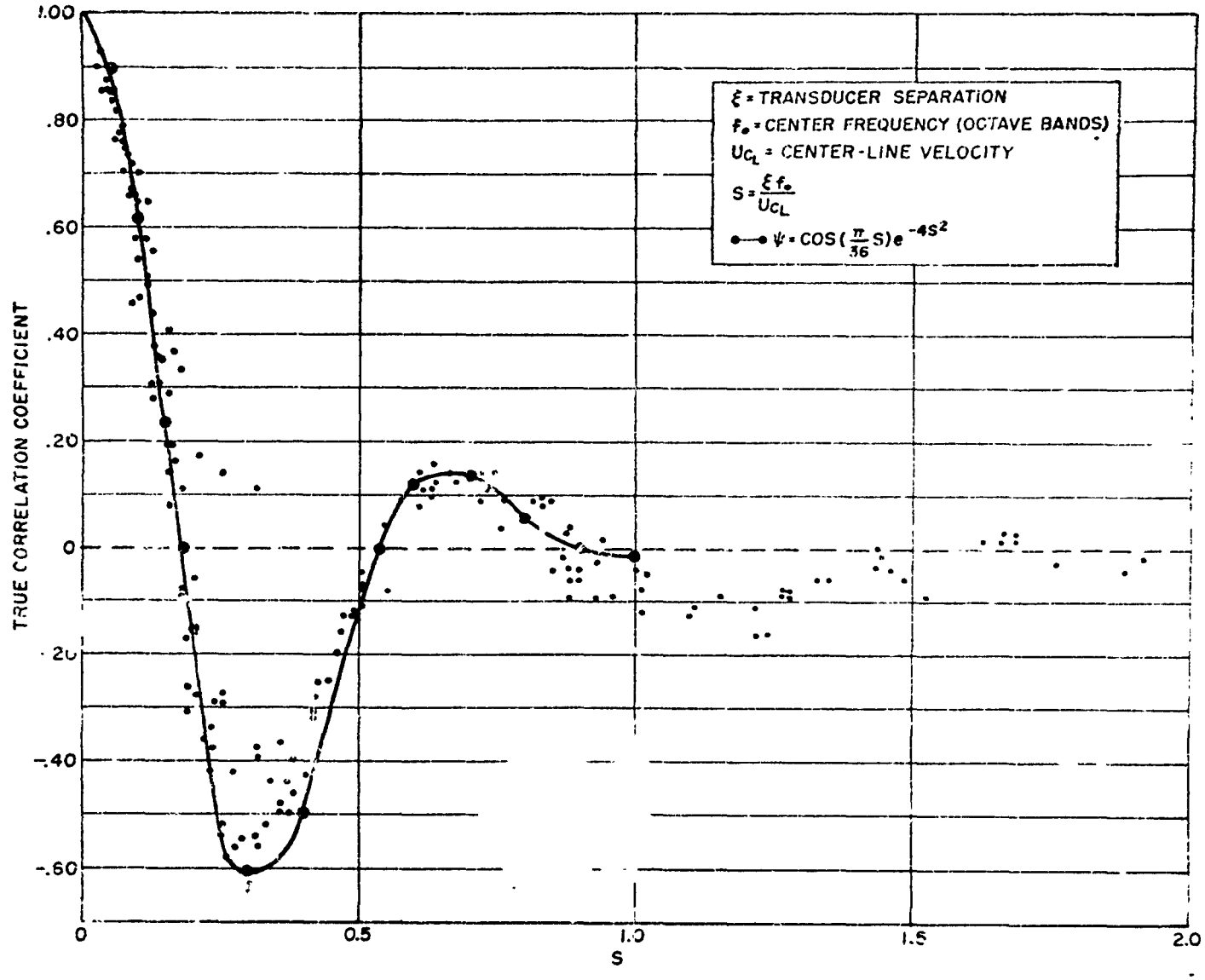

Fig. 28 - Longitudinal Correlation versus Strouhal Number Based on Centerline Velocity

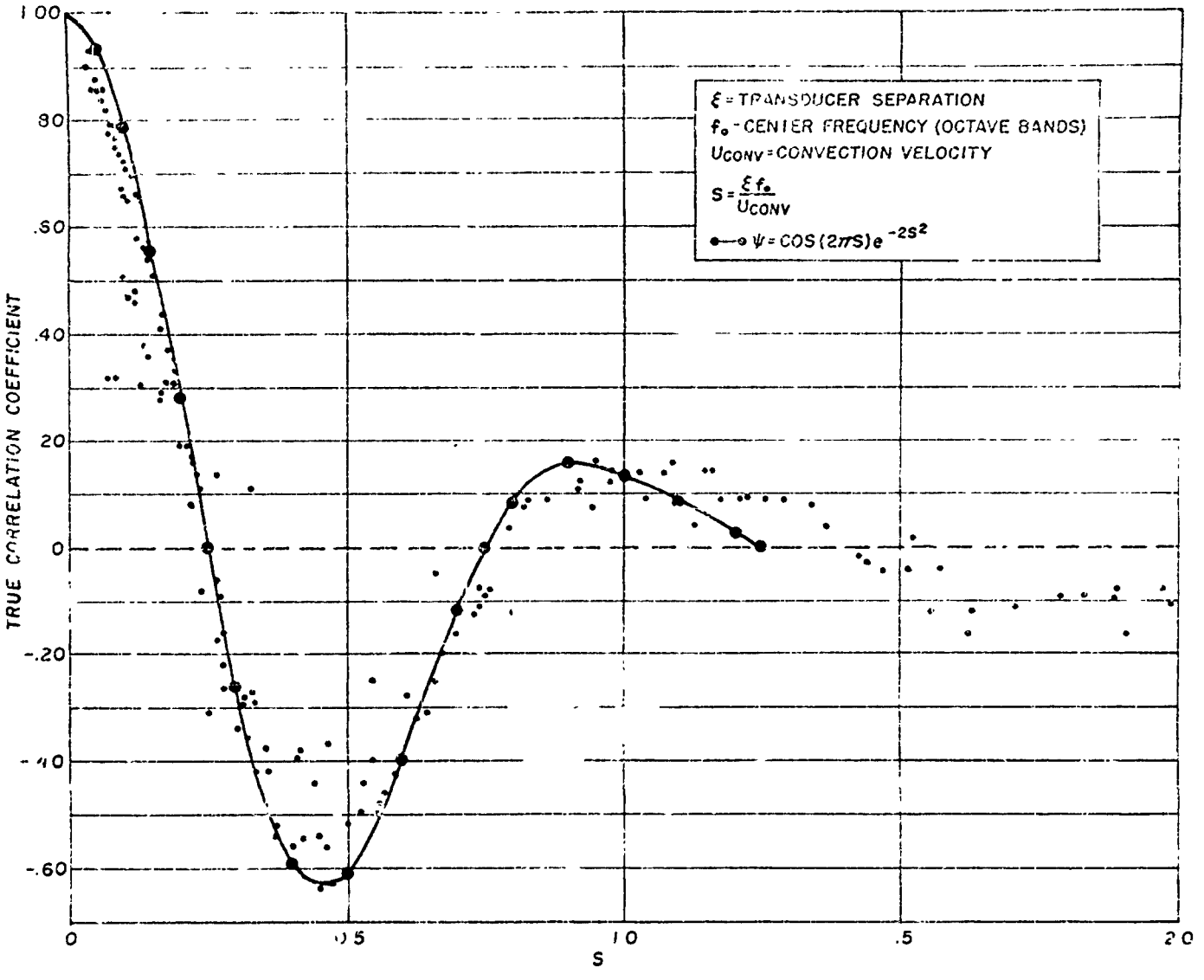

Fig. 29 - Longitudinal Correlation versus Strouhal Number Based on Convection Velocity

Fig. 29 - Longitudinal Correlation versus Strouhal Number Based on Convection Velocity

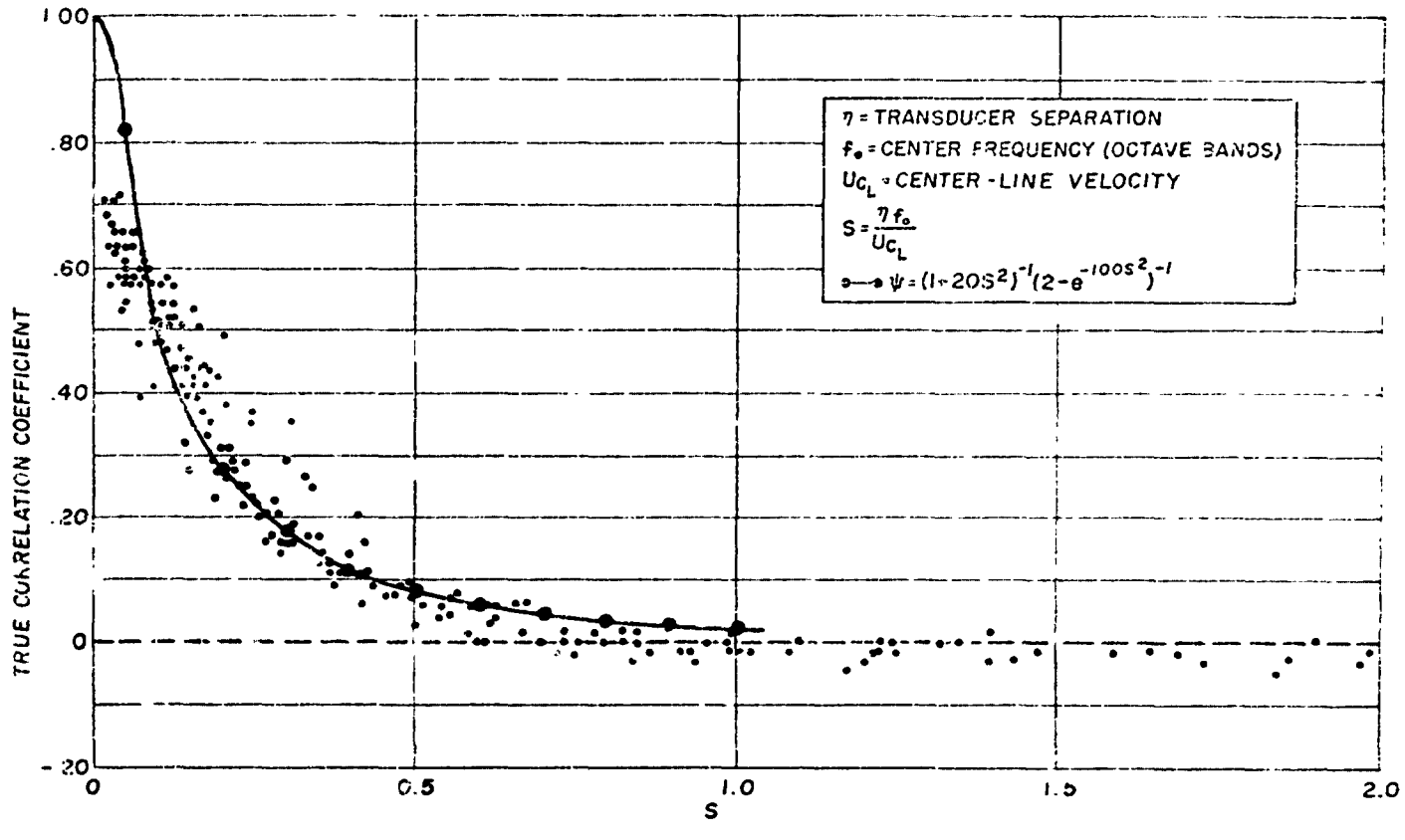

Fig. 30 - Lateral Correlation versus Strouhal Number Based on Centerline Velocity

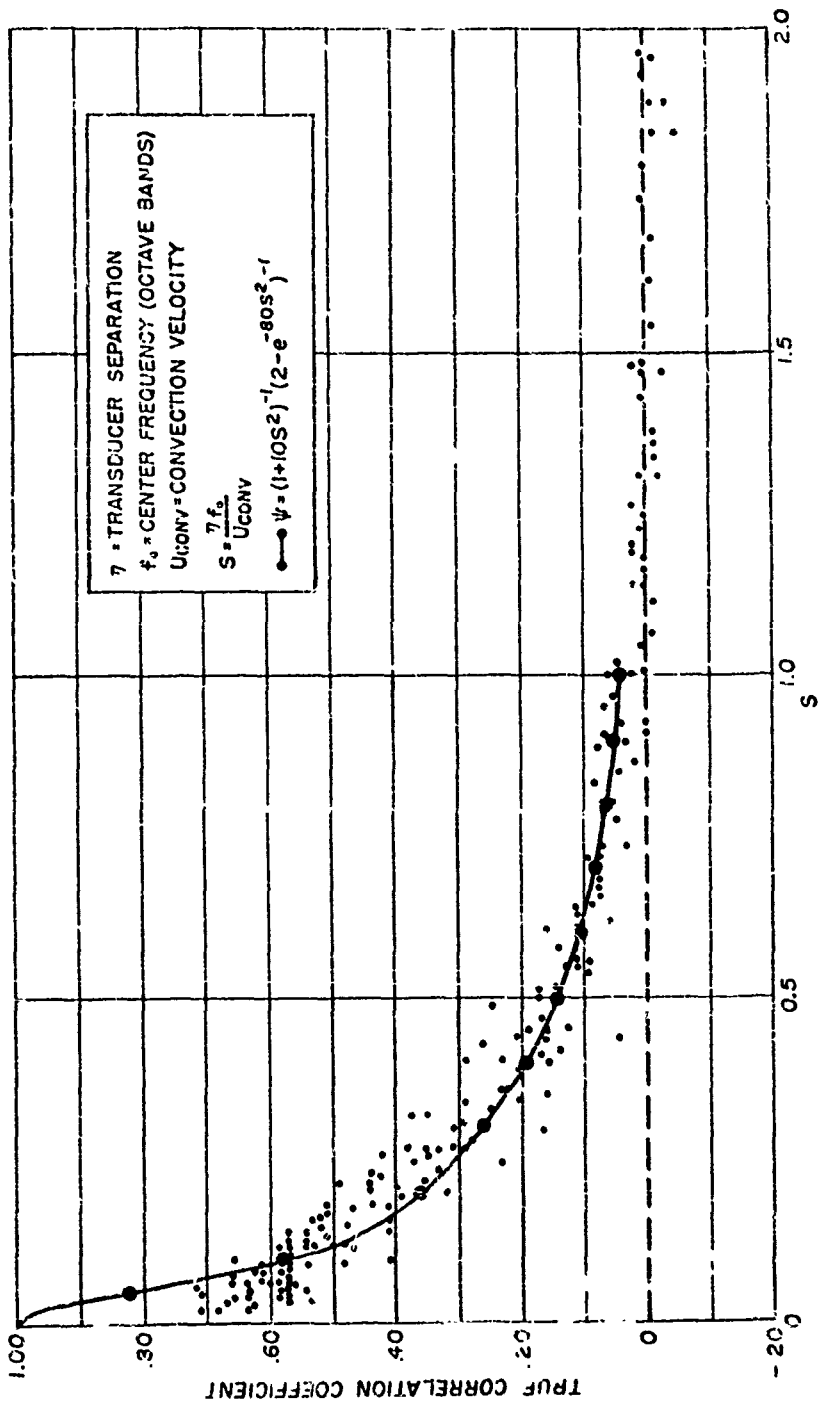

Fig. 31 - Lateral Correlation versus Strouhal Number Based on Convection Velocity

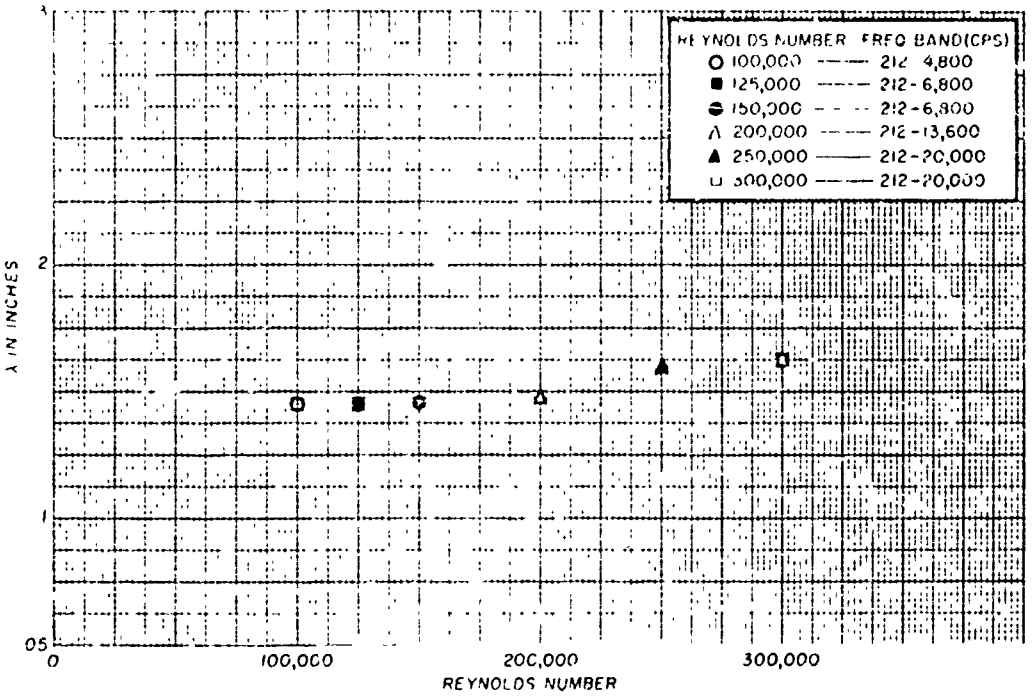

Fig. 32 - Estimate of the Longitudinal Scale

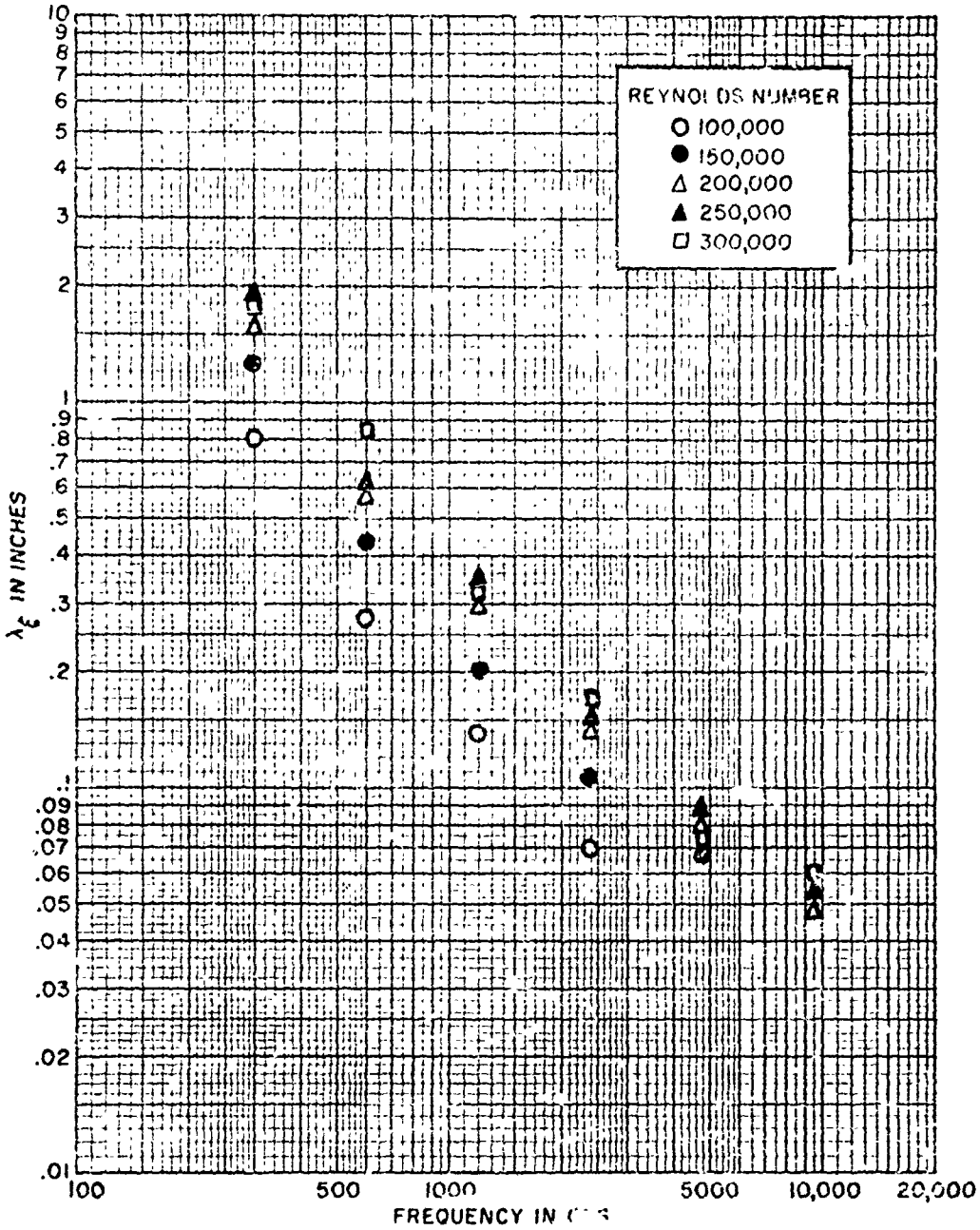

Fig. 33 - Estimate of the Longitudinal Scale versus Frequency (Based on Auto-correlation Data)

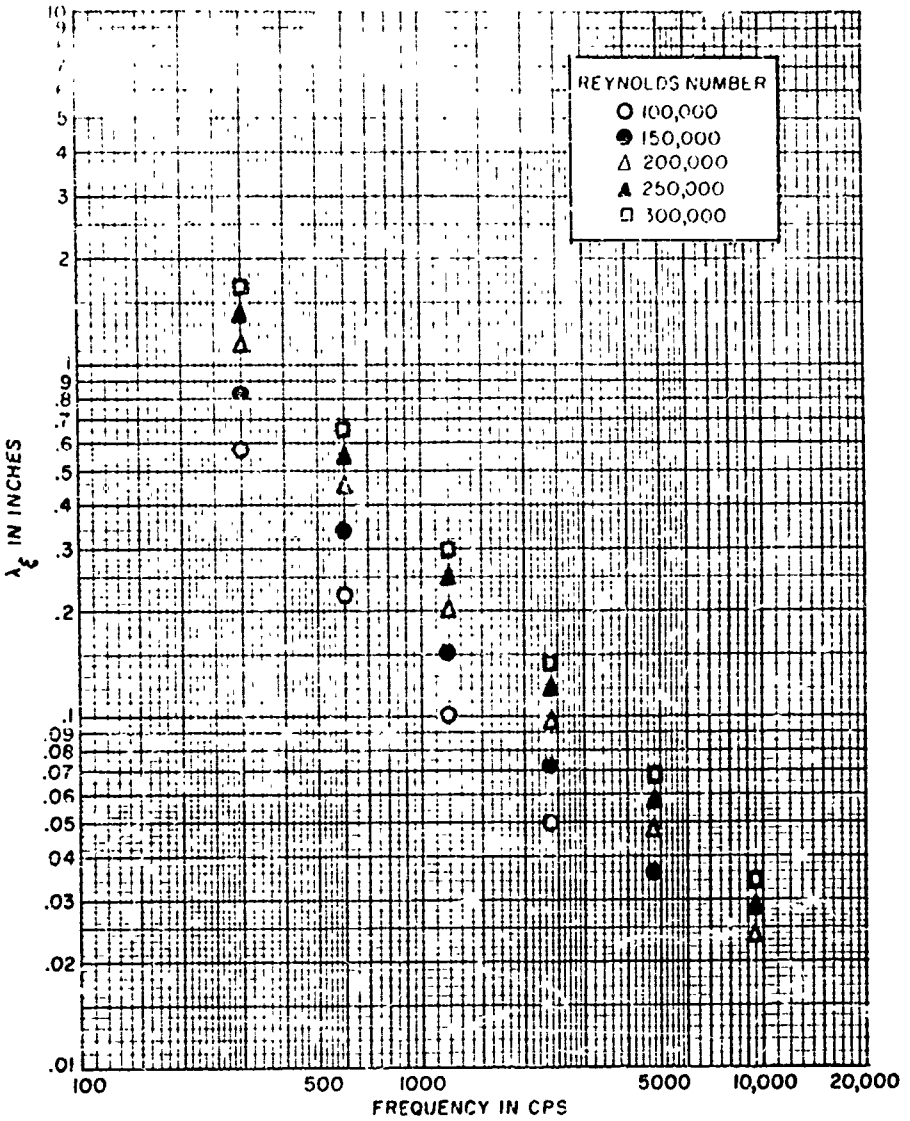

Fig. 34 - Estimate of the Longitudinal Scale versus Frequency
(Based on Correlation Data as a Function of Strouhal Number)

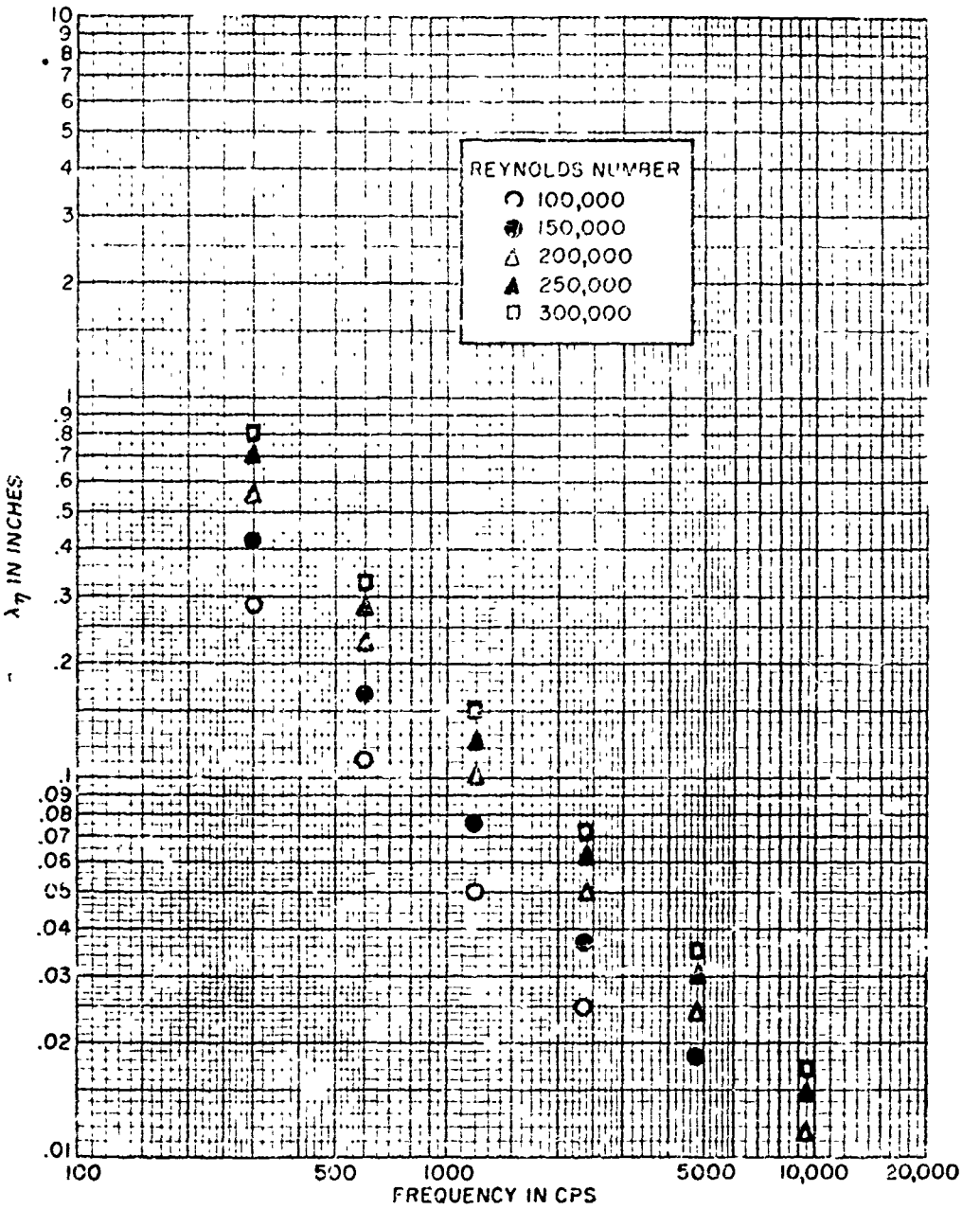

Fig. 35 - Estimate of the Lateral ... versus Frequency
(Based on Correlation Data as a Function of Strouhal Number)

ABSTRACT CARD LAYOUT
SND-USNUSL-222

SND-P&PO-5959

Navy Underwater Sound Laboratory
Report No. 559
WALL PRESSURE CORRELATIONS IN TURBULENT PIPE FLOW by Henry P. Bakewell, Jr., George F. Carey, John J. Libuha, Howard H. Schloemer, and William A. Von Winkle, 20 August 1962, i-iv + 50 pp., figs.
UNCLASSIFIED

Certain properties of the pressure field induced by turbulent airflow at the wall of a cylindrical pipe have been investigated over broad frequency bands and in octave frequency bands over a limited range of Reynolds numbers. The broad-band measurements indicate that the pressure field is convected downstream at approximately 0.7 of the centerline velocity. The ratio of the root-mean-square pressure to the dynamic pressure is approximately equal to 0.006 for the various Reynolds numbers. Longitudinal and lateral space correlations are also presented for a limited range of spatial separations. Data obtained in octave frequency bands indicate that the ratio of convection velocity to centerline velocity decreases as frequency increases, with the ratio varying from approximately unity to 0.64 for the frequency bands investigated. Longitudinal and lateral correlation data for various frequencies, spatial separations, and Reynolds numbers are shown to be functions of Strouhal number. Estimates of the longitudinal and lateral scales are given as functions of frequency for the various Reynolds numbers. These data indicate that the lateral scale is approximately equal to one half of the longitudinal scale.

1. Turbulent flow
2. Turbulent boundary layer
3. Cylinders—Pressure distribution—Measurement
I. Bakewell, Henry P., Jr.
II. Carey, George F.
III. Libuha, John J.
IV. Schloemer, Howard H.
V. Von Winkle, William A.
VI. Title
VII. S-R011 01 01-0401

Navy Underwater Sound Laboratory
Report No. 559
WALL PRESSURE CORRELATIONS IN TURBULENT PIPE FLOW by Henry P. Bakewell, Jr., George F. Carey, John J. Libuha, Howard H. Schloemer, and William A. Von Winkle 20 August 1962, i-iv + 50 pp., figs.
UNCLASSIFIED

Certain properties of the pressure field induced by turbulent airflow at the wall of a cylindrical pipe have been investigated over broad frequency bands and in octave frequency bands over a limited range of Reynolds numbers. The broad-band measurements indicate that the pressure field is convected downstream at approximately 0.7 of the centerline velocity. The ratio of the root-mean-square pressure to the dynamic pressure is approximately equal to 0.006 for the various Reynolds numbers. Longitudinal and lateral space correlations are also presented for a limited range of spatial separations. Data obtained in octave frequency bands indicate that the ratio of convection velocity to centerline velocity decreases as frequency increases, with the ratio varying from approximately unity to 0.64 for the frequency bands investigated. Longitudinal and lateral correlation data for various frequencies, spatial separations, and Reynolds numbers are shown to be functions of Strouhal number. Estimates of the longitudinal and lateral scales are given as functions of frequency for the various Reynolds numbers. These data indicate that the lateral scale is approximately equal to one half of the longitudinal scale.

1. Turbulent flow
2. Turbulent boundary layer
3. Cylinders—Pressure distribution—Measurement
I. Bakewell, Henry P., Jr.
II. Carey, George F.
III. Libuha, John J.
IV. Schloemer, Howard H.
V. Von Winkle, William A.
VI. Title
VII. S-R011 01 01-0401

Navy Underwater Sound Laboratory
Report No. 559

WALL PRESSURE CORRELATIONS IN TURBULENT PIPE FLOW by Henry P. Bakewell, Jr., George F. Carey, John J. Libuha, Howard H. Schloemer, and William A. Von Winkle, 20 August 1962, i-iv + 50 pp., figs.

UNCLASSIFIED

Certain properties of the pressure field induced by turbulent airflow at the wall of a cylindrical pipe have been investigated over broad frequency bands and in octave frequency bands over a limited range of Reynolds numbers. The broad-band measurements indicate that the pressure field is convected downstream at approximately 0.7 of the centerline velocity. The ratio of the root-mean-square pressure to the dynamic pressure is approximately equal to 0.006 for the various Reynolds numbers. Longitudinal and lateral space correlations are also presented for a limited range of spatial separations. Data obtained in octave frequency bands indicate that the ratio of convection velocity to centerline velocity decreases as frequency increases, with the ratio varying from approximately unity to 0.64 for the frequency bands investigated. Longitudinal and lateral correlation data for various frequencies, spatial separations, and Reynolds numbers are shown to be functions of Strouhal number. Estimates of the longitudinal and lateral scales are given as functions of frequency for the various Reynolds numbers. These data indicate that the lateral scale is approximately equal to one half of the longitudinal scale.

1. Turbulent flow
2. Turbulent boundary layer
3. Cylinders—Pressure distribution—Measurement
I. Bakewell, Henry P., Jr.
II. Carey, George F.
III. Libuha, John J.
IV. Schloemer, Howard H.
V. Von Winkle, William A.
VI. Title
VII. S-R011 01 01-0401

Navy Underwater Sound Laboratory
Report No. 559

WALL PRESSURE CORRELATIONS IN TURBULENT PIPE FLOW by Henry P. Bakewell, Jr., George F. Carey, John J. Libuha, Howard H. Schloemer, and William A. Von Winkle, 20 August 1962, i-iv + 50 pp., figs.

UNCLASSIFIED

Certain properties of the pressure field induced by turbulent airflow at the wall of a cylindrical pipe have been investigated over broad frequency bands and in octave frequency bands over a limited range of Reynolds numbers. The broad-band measurements indicate that the pressure field is convected downstream at approximately 0.7 of the centerline velocity. The ratio of the root-mean-square pressure to the dynamic pressure is approximately equal to 0.006 for the various Reynolds numbers. Longitudinal and lateral space correlations are also presented for a limited range of spatial separations. Data obtained in octave frequency bands indicate that the ratio of convection velocity to centerline velocity decreases as frequency increases, with the ratio varying from approximately unity to 0.64 for the frequency bands investigated. Longitudinal and lateral correlation data for various frequencies, spatial separations, and Reynolds numbers are shown to be functions of Strouhal number. Estimates of the longitudinal and lateral scales are given as functions of frequency for the various Reynolds numbers. These data indicate that the lateral scale is approximately equal to one half of the longitudinal scale.

1. Turbulent flow
2. Turbulent boundary layer
3. Cylinders—Pressure distribution—Measurement
I. Bakewell, Henry P., Jr.
II. Carey, George F.
III. Libuha, John J.
IV. Schloemer, Howard H.
V. Von Winkle, William A.
VI. Title
VII. S-R011 01 01-0401

ABSTRACT CARD LAYOUT
3ND-USNUSL-232

3ND-P&PO-5939

Navy Underwater Sound Laboratory
Report No. 559
WALL PRESSURE CORRELATIONS IN TURBULENT PIPE FLOW by Henry P. Bakewell, Jr., George F. Carey, John J. Libuha, Howard H. Schloemer, and William A. Von Winkle, 20 August 1962, i-iv + 50 pp., figs.
UNCLASSIFIED

Certain properties of the pressure field induced by turbulent airflow at the wall of a cylindrical pipe have been investigated over broad frequency bands and in octave frequency bands over a limited range of Reynolds numbers. The broad-band measurements indicate that the pressure field is convected downstream at approximately 0.7 of the centerline velocity. The ratio of the root-mean-square pressure to the dynamic pressure is approximately equal to 0.006 for the various Reynolds numbers. Longitudinal and lateral space correlations are also presented for a limited range of spatial separations. Data obtained in octave frequency bands indicate that the ratio of convection velocity to centerline velocity decreases as frequency increases, with the ratio varying from approximately unity to 0.64 for the frequency bands investigated. Longitudinal and lateral correlation data for various frequencies, spatial separations, and Reynolds numbers are shown to be functions of Strouhal number. Estimates of the longitudinal and lateral scales are given as functions of frequency for the various Reynolds numbers. These data indicate that the lateral scale is approximately equal to one half of the longitudinal scale.

1. Turbulent flow
2. Turbulent boundary layer
3. Cylinders—Pressure distribution—Measurement
I. Bakewell, Henry P., Jr.
II. Carey, George F.
III. Libuha, John J.
IV. Schloemer, Howard H.
V. Von Winkle, William A.
VI. Title
VII. S-R011 01 01-0401

Navy Underwater Sound Laboratory
Report No. 559
WALL PRESSURE CORRELATIONS IN TURBULENT PIPE FLOW by Henry P. Bakewell, Jr., George F. Carey, John J. Libuha, Howard H. Schloemer, and William A. Von Winkle, 20 August 1962, i-iv + 50 pp., figs.
UNCLASSIFIED

Certain properties of the pressure field induced by turbulent airflow at the wall of a cylindrical pipe have been investigated over broad frequency bands and in octave frequency bands over a limited range of Reynolds numbers. The broad-band measurements indicate that the pressure field is convected downstream at approximately 0.7 of the centerline velocity. The ratio of the root-mean-square pressure to the dynamic pressure is approximately equal to 0.006 for the various Reynolds numbers. Longitudinal and lateral space correlations are also presented for a limited range of spatial separations. Data obtained in octave frequency bands indicate that the ratio of convection velocity to centerline velocity decreases as frequency increases, with the ratio varying from approximately unity to 0.64 for the frequency bands investigated. Longitudinal and lateral correlation data for various frequencies, spatial separations, and Reynolds numbers are shown to be functions of Strouhal number. Estimates of the longitudinal and lateral scales are given as functions of frequency for the various Reynolds numbers. These data indicate that the lateral scale is approximately equal to one half of the longitudinal scale.

1. Turbulent flow
2. Turbulent boundary layer
3. Cylinders—Pressure distribution—Measurement
I. Bakewell, Henry P., Jr.
II. Carey, George F.
III. Libuha, John J.
IV. Schloemer, Howard H.
V. Von Winkle, William A.
VI. Title
VII. S-R011 01 01-0401

INITIAL DISTRIBUTION LIST

ONR, Code 411
" " 468
OpNav (Op-07T) (2)
BuShips, Code 320
" " 330
" " 333
" " 335 (3)
" " 345 (2)
" " 525
" " 688 (2)
BuWeps, Code RU
ComOpTevFor
ComOpTevFor, Undersea Warfare Division
CO, USNOS, Newport
CO and Dir., DTMB
CO and Dir., USNEL
CO, U. S. Navy Mine Defense Laboratory

Com, NOL
Com, US NOTS, China Lake
Com, US NOTS, Pasadena Annex
Dir., NRL
Dir., ORL
Dir., WHOI
Dir., Acoustics Research Laboratory
Harvard University
Applied Physics Laboratory, University
of Washington (via INSMAT, Code 1051, Seattle)
Hudson Laboratories, Dobbs Ferry
President, Naval War College
Superintendent, USN PG School
Dir., Systems Analysis Group, R and D
Planning Council, NOL
ASTIA, Document Service Center (10)
CO, ONR, London Branch